Design, Fabrication, and Characterization

of a Wideband Microwave Balun

by

Shu Lu

Thesis submitted to the faculty of the

Virginia Polytechnic Institute and State University

in partial fulfillment of the requirements for the degree of

Master of Science

in

Electrical Engineering

APPROVED:

Aicha Elshabini-Riad

Dr. Aicha Elshabini-Riad,

Sedki M. Riad

Dr. Sedki M. Riad,

Co-Chairpersons.

Warren L. Stutzman

Dr. Warren L. Stutzman

April, 1990

Blacksburg, Virginia

Design, Fabrication, and Characterization of a Wideband Microwave Balun

by

Shu Lu

A. Elshabini-Riad, S.M. Riad, Co-Chairpersons

Electrical Engineering

(ABSTRACT)

A wideband microwave balun is designed to adapt unbalanced to balanced transmission line networks. The balun is realized by a planar microstrip line configuration on a double copper cladded teflon-ceramic composite board. The microstrip line conductor pattern was formed on the board using the chemical etching process. The fabricated balun is measured and evaluated in both the time domain and frequency domain, indicating a 5 GHz bandwidth. The time domain modeling technique is used to characterize the balun's performance. Based on physical analysis of the balun's configuration, the discontinuities through the transmission paths are modeled as distributed and lumped elements, resulting in an equivalent network model for the balun structure. The obtained model successfully simulates the balun's performance.

Acknowledgements

I would like to take this opportunity to thank everyone who has helped me in finishing this thesis. Particularly, I would like to express my gratitude and appreciation to professors Aicha Elshabini-Riad and Sedki M. Riad for their effort and time spent on technical guidance, discussion, and help so that I can complete this thesis.

I would like to extend my thanks to Dr. W.L. Stutzman for providing useful information, helpful suggestions and for serving on my thesis committee.

I would also like to thank Mr. Wansheng Su and Mr. Monty B. Hayes for their valuable technical discussion and suggestions, which are great help for me to finish the thesis work.

I deeply wish to thank my parents for their unfailing love and continuous support, without which this thesis could not have been completed. I finally thank my husband, Jianqing He, for his understanding and assistance in many ways, which are necessary to the successful completion of the thesis.

This work was performed at the Time Domain Lab, with fabrication work done at the Hybrid Microelectronics Lab.

CONTENTS

List of Illustrations

CHAPTER I

INTRODUCTION

In many microwave applications, baluns are used for converting signal's configurations from unbalanced to balanced and vice versa. Signal configuration conversion can be classified into two categories: a) from an unbalanced input into two balanced outputs; b) from an unbalanced input into two unbalanced outputs. The two outputs from a balun are characterized by having equal amplitudes with opposite phases (antiphases).

Baluns can be used in a variety of applications such as dipole antenna, balanced mixers, and phase detectors, etc. Other applications involve splitting pulses from a pulse generator into a pair of equal but opposite polarity pulse. For example, in a dipole antenna, a pair of balanced currents with respect to the ground is needed. In order to produce the balanced currents, a balun is used to transform the unbalanced input from the source to a balanced pair of signals to feed the dipole antenna. Another example is that of the travelling wave oscilloscope where a signal is fed into the 50 Ω input, which is to be split into push-pull signals for directly driving the two 100 Ω deflection plates of the CRT. An example for balun application for pulse splitting is the case of a balanced time domain reflectometer where the test probe is balanced while the TDR unit itself is unbalanced.

Baluns can have different configurations such as transmission line baluns and transformer baluns. They can be designed for one frequency (CW application) or for applications requiring a wideband frequency range (e.g. transient). As an example, a split coaxial balun is designed for CW application [1]. It is realized by connecting an extra quater-wavelength of coaxial to the outer conductor of the main transmission line. For wideband applications, both transformer baluns and transmission line baluns can be used.

Transformer baluns provide a pair of balanced signals at the secondary winding, the signals are coupled from the primary winding by magnetic field. Nishiauka, Sato, Nakatsuyama and Nagahashi introduced a very-wide-band balun transformer which has a bandwidth from 20 MHz to 500 MHz [2]. This balun transformer has better high frequency response than the isolation-type balun transformer [2]. Its high frequency response is achieved by inserting a certain phase shift to compensate the 90° phase shift of the winding length.

Transmission Line balun usually consists of a power splitter and a phase reversal junction. The most common balun, named compensated balun, was described and analyzed in [3-8]. The basic idea of the compensated balun is that the signal line of the unbalanced input is fed to a quater wavelength short-circuit stub at the balun junction. The short-circuit stub possesses the functions of a power splitter and a phase reversal junction. Bawer and Wolfe subsequently applied the compensated balun to a broadband spiral antenna which had a frequency range from about 2 GHz to 4 GHz [9]. Laughlin designed a new impedance-matched wide-band compensated balun which showed a bandwidth from 2 GHz to 4 GHz [10]. A printed dipole radiating element with an integrated microstip compensated balun was described by Edward and Rees [11]. The balun featured a broad operating bandwidth from 11 GHz to 16 GHz. Recently, an integrated circuit 2-18 GHz balun is reported [12]. This wideband balun is realized by two parts; a two-way power splitter to produce two outputs with equal amplitudes, and a phase shifter to obtain 180 degree difference. The phase shifter consists of two bandpass circuits; one circuit is a coupled line pair while the other circuit is a pi-network made up of three sections of transmission line.

The great concern in the design and the realization of a wideband balun has been in the bandwidth limitation. In addition, the device size becomes important in order to incorporate a balun into a compact instrument and a small size part. A commercially produced transmission line balun by Picosecond Pulse Labs (Model No. 5420) possesses a broad spectrum with a bandwidth extending from 5 kHz to X band; but it has relatively large size [13]. Another commercially available RF pulse transformer balun Adam-Russel TP 101 has a typical bandwidth of 500 kHz to 1.5 GHz although it has an advantage of small size [14].

Design of a high quality wideband transmission line balun concentrates on two major factors: phase reversal junction and impedance matching. The antiphase is obtained at the junction, at which the signal conductor is exchanged with the common ground. Such a reversal junction usually produces an effect on the low cutoff frequency. An impedance matching network is often necessary in order to match the impedance of the input transmission line to that of the output transmission lines. The impedance matching network is the main limiting factor for high frequency cutoff of the balun.

In the research conducted in this thesis, planar stripline baluns are designed and realized on teflon-ceramic composite substrates using the hybrid technology. The resulting microstrip line balun possesses various advantages including a broadband (from 2.46 MHz to 5 GHz when 3-foot long testing cables are connected on the balun outputs), small size, and low cost. The topics studied in this thesis include the following:

1. Investigation of the factors limiting the bandwidth of the balun.

2. Design a wideband balun using planar transmission lines.

3. Realization of a wideband balun using the hybrid technology.

4. Characterization and modeling of a microstrip line balun.

The constructed baluns are measured and evaluated in both frequency domain and time domain. In the frequency domain, the frequency dependent S-parameters are usually tested and evaluated. In the time domain, both time domain reflection (TDR) and time domain transmission (TDT) are used for measurement and guidance of the design.

The thesis is written in the following arrangement. Chapter 1 is a general introduction. The next chapter, Chapter 2, introduces the basic balun concept and presents possible approaches to realize baluns. In Chapter 3, design considerations of hybrid baluns are discussed. The realization of the designed baluns using hybrid technology is described. Chapter 4 covers the measurement techniques and the results are evaluated. In chapter 5, the process of characterization and modeling of the microstrip line balun is described in details, and the obtained model is presented. Finally, conclusions of the work are provided in Chapter 6.

CHAPTER II

BALUN CONCEPT

2.1. Basic Balun Concept

A microwave balun is a term used by antenna engineers to describe a device which transforms an unbalanced to a balanced transmission line. In many microwave applications such as a dipole antenna, a magic tee and a probe used for transmitting a pair of electromagnetic pulses, it is desirable to have two output signals, excited from the same source, identical in electrical parameters with 180-degree phase difference from each other. This basic concept of a balun can be demonstrated in a schematic as shown in Figure 2.1. An input signal is fed via a transmission line into an impedance matching network, consisting of three 16.67 Ω resistors for the case of 50 Ω transmission line. The network is basically a 6-dB power splitter, at which the input signal is then split into two secondaries. The polarity of one of the secondaries is reversed by exchanging the contacts of the signal line and the ground plane. The other secondary is left unaltered. The reversed polarity secondary signal is identical to the other one except for its phase, which is 180 degrees different. These two signals are then extended to the outputs through 50 Ω transmission lines.

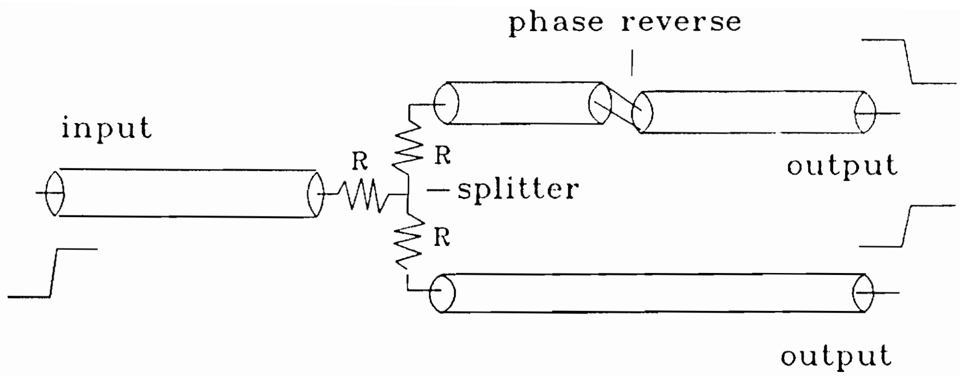

Figure 2.1 Basic Idea of The Balun

Intuitive observation of the shown configuration of balun can locate two inherent discontinuities through which the input signal is propagated from the input terminal to the phase-reversed output terminal. One discontinuity is introduced by the matching network while the other is caused by the phase reversal junction. The phase reversal junction plays an important role in achieving a wide bandwidth since the field is severely disturbed at the junction.

2.2. Transformer Balun

A RF transformer can produce two secondary signals with antiphase and equal amplitude from the same source. A configuration of a transformer balun is shown in Figure 2.2. As mentioned before, the main disadvantage of the transformer balun is its limited bandwidth. This can be attributed to the frequency characteristics of a transformer. It has been known that the mutual inductance of a transformer is proportional to the rate of the current variation with time. This inherent feature determines the poor low frequency characteristics of the transformer. At DC the transformer acts as an open. The high frequency characteristics are primarily determined by two factors. The first factor is the loss of the ferromagnetic materials at high frequency. This loss becomes quite significant as frequency goes into the range of GHz. So far, ferromagnetic materials with good high frequency characteristics have not been found. The second factor limiting high frequency characteristics is the skin effect. As the operating frequency becomes higher, the effective conductors of the coils become smaller due to skin effect. Power dissipation is increased due to the increase of the resistance with the frequency, resulting in great loss within

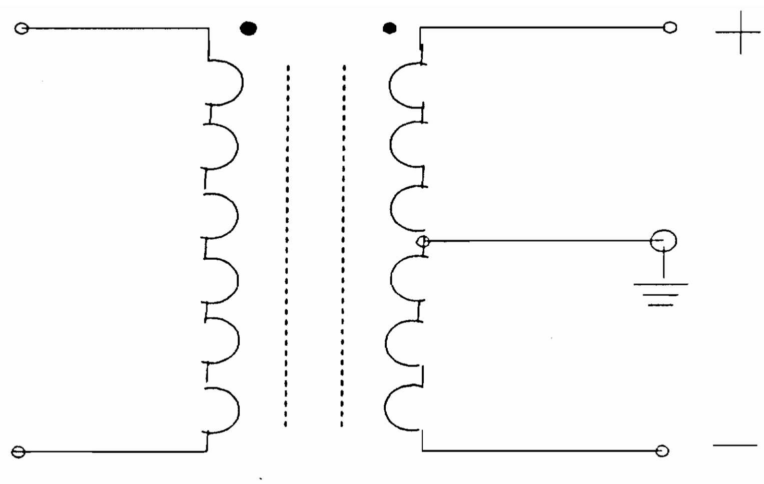

Figure 2.2 Transformer Balun

the transformer. The losses from these two sources set the limitation of the high frequency characteristics of the transformer. As a typical example, an RF Pulse Transformer Balun, made by Adams-Russell Anzac Division, has a bandwidth of 500 kHz - 1.5 GHz [3].

2.3 Typical Application

An example is given to illustrate an application of the balun concept. It is known that the dielectric constant of soil varies as the content (percentage) of water in the soil changes. Based on this fact, an instrument for determining soilmoisture is designed using Time Domain Reflectometry (TDR) technique. A step pulse is transmitted into the soil through a microwave probe, which consists of two metal bars and is to be inserted into the soil. Analyzing the reflection waveform, the dielectric constant can be determined, thus the water content in the soil can be determined. In order to obtain a symmetrical configuration of the electromagnetic field in the probe, the step pulse needs to be splitted into two signals which are identical in magnitude and 180-degree different in phase before it goes into the probe. Therefore, a balun is needed in such an application. A transformer balun is used in the instrument. Because of its limited bandwidth, the transformer balun limits the performance of the instrument. If the transformer balun is replaced by the balun made by Picosecond Pulse Labs [14], the instrument's performance can be greatly improved due to its wide bandwidth. However, it is large in size so that its use in such an instrument is not practical. This drawback in the instrument motivates the idea to design and fabricate a wideband balun in a miniature size.

2.4 Coaxial Cable Experiment

The possibility of using transmission lines to construct a balun necessitates understanding the phenomena occurring when the phase of the signal is changed. A simple way to achieve that task is to conduct a coaxial cable experiment. Such an experiment helps to develop an insight of the balun design and its performance parameters. The reason of selecting coaxial cable is that the only non-standard element in the coaxial cable components is the phase reversal section so that the analysis involved becomes simple. Two pieces of coaxial cables were connected in cascade such that the outer conductor of the second cable was connected to the inner conductor of the first cable and vice versa. Figure 2.3 illustrates the configuration of the cable connection.

A step voltage was then applied to the first cable and the Time Domain Reflection (TDR) waveform is shown in Figure 2.4. It is observed that the characteristic impedance of the second cable appears less than its actual value of 50 Ω. It is interesting to analyze this phenomenon. Considering the distribution of the electromagnetic field within the coaxial cables, one can realize the difference of the field distribution between the first cable and the second one. Within the first cable, there is no field leakage because the field is basically confined between the inner conductor and the outer conductor. On the other hand, the field distribution is different within the second cable because the inner conductor becomes the ground while the outer conductor is actually the signal line after the phase reversal junction. A physical explanation of the drop in characteristic impedance in the second cable can be provided. It is also

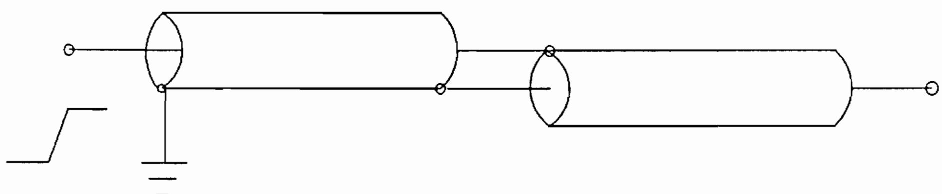

Figure 2.3 Phase Reversal Experiment

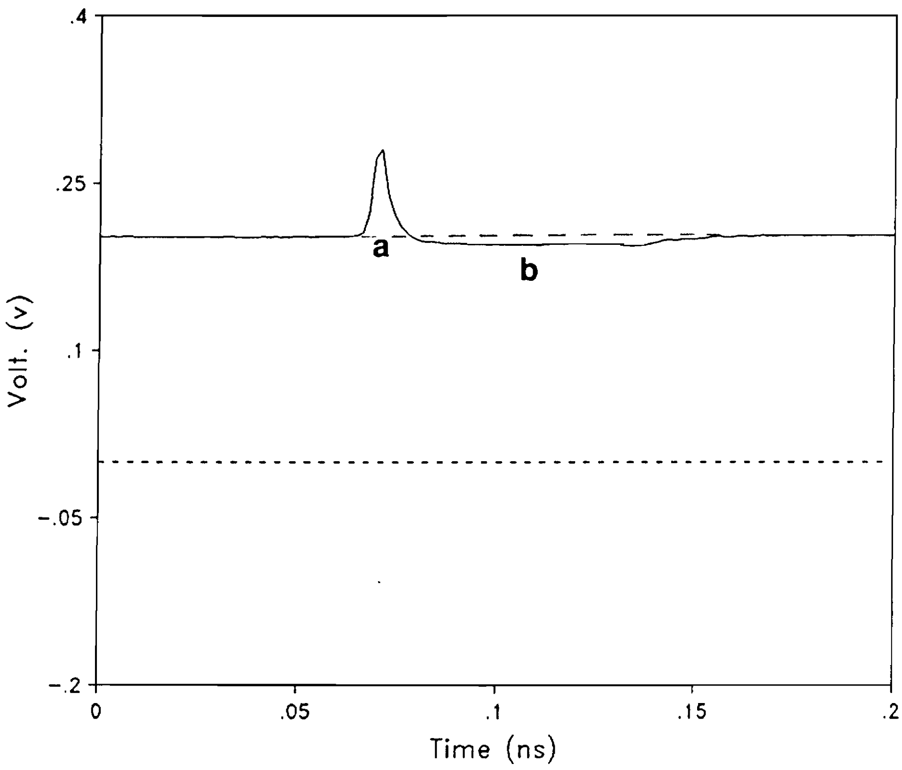

a __ Reversal junction
b __ Impedance drop

Figure 2.4 TDR Waveform of The Cascade Coaxial Cable With Its Inner and Outer Conductor Exchanged at the Junction

observed that the TDR waveform is distorted at the phase reversal junction. The performance of this coaxial junction is greatly dependent on its impedance discontinuity. The smaller the disturbance and the junction size, the better the high frequency performance of the cascaded cables.

Two important conclusions are derived from the coaxial cable experiment. The first is that it is necessary to achieve a smooth transition at the phase reversal junction in order to minimize the discontinuity. And the second is related to the impedance drop at the junction. To remedy such drop, the characteristic impedance of the transmission line can be designed to compensate for the impedance difference.

2.5. Hybrid Transmission Line Approach

The commonly used transmission lines include coplanar lines and microstrip lines. These transmission lines can be realized using hybrid technologies, such as conventional thick film printing and copper cladded teflon-ceramic composite substrates that can be chemically etched. The hybrid transmission lines possess advantages of wideband frequency performance, simple fabrication and geometrical manipulation, as well as low cost. A coplanar line realized on 96% aluminum substrate using thick film technology, has exhibited good frequency performance up to 10 GHz [15]. This wideband characteristic of the planar transmission lines provides possibilities to realize wideband baluns on substrates using planar transmission lines. Since the process of balun realization involves an optimization of the balun's performance through iterative modification of the dimensions of the line, hybrid methods represent good candidates to accomplish such process. In particular, multilayer hybrid technology, such as Green Tape, may incorporate a balun realized by a planar transmission line into small size hybrid microwave integrated circuits and other portable instruments.

The way to realize the phase reversal junction involved in design of a balun is a main critical concern to achieve success. In order to realize the phase reversal junction, jumpers have to be used for the junction on the coplanar line while the junction on the microstrip line can be made only by manipulating proper dimensions for the upper conductor plane and the bottom conductor plane. It is expected that the junction on the microstrip line introduces less disturbance than the one on the coplanar line due to different field distributions. More detailed explanation will be provided in Chapter 2.

2.6. Conclusion

The basic concept of a balun is introduced in this Chapter. Several ways to realize a balun are described. Although an RF transformer is a simple way to realize the balun, its poor bandwidth gives rise to great limitation to the bandwidth of the transformer balun. The wideband characteristics of planar transmission lines such as coplanar lines and microstrip lines provide preferable choice for a wideband balun. Preliminary experiments on coaxial cable are conducted in order to understand the problems occurring during the design of the balun. The conclusions derived from the results of the experiments indicate that discontinuities and impedance drop introduced by the phase reversal junction are critical factors to be resolved in order to realize a wideband balun.

CHAPTER III

BALUN DESIGN AND FABRICATION

3.1. Introduction

In this chapter, design and fabrication of two baluns are described. The first balun is a coplanar line balun, and the second balun is a microstrip line balun. Because of the difference in geometrical configuration between the coplanar line and the microstrip line, different design considerations are observed. Design of the phase reversal junction is particularly important in order to introduce less field disturbance at the junction. The designed baluns are fabricated by chemical etching of copper cladded ceramics.

3.2. Characteristics of Planar Transmission Lines

The most commonly used planar transmission lines fabricated using the hybrid technology processing are the microstrip lines and the coplanar lines. Because of their convenient compatibilities to hybrid microwave circuits, they have been widely used in microwave circuits.

3.2.1. Microstrip Transmission Line

A microstrip line is a two-conductor transmission line, as shown in Figure 3.1. Parameters that determine the line's characteristics are top conductor strip width 'W', thickness 't' of conductor, dielectric substrate thickness 'H', and relative dielectric constant 'ϵ_r' of the substrate. It has been known that a pure TEM propagation mode cannot be supported in a microstrip line due to the presence of the air-dielectric interface. The modes propagated include non-TEM hybrid modes (as compared with a pure TEM-mode in stripline). However, it can be approximately treated as a pure TEM mode for a simple analysis. This is known as quasi-static analysis method, which can lead to closed-form expressions greatly necessary for optimization and computer-aided design. The closed-form expressions of characteristic impedance Z_0 and effective dielectric constant ϵ_{eff} are given by [16],

For $W/H \geq 1$,

$$Z_0 = \frac{120\ \pi/\sqrt{\epsilon_{eff}}}{W_e/H + 1.393 + 0.667\ \ln(W_e/H+1.444)} \qquad (1)$$

$$\epsilon_{eff} = \frac{\epsilon_r+1}{2} + \frac{\epsilon_r-1}{2}\left(1 + 12H/W_e\right)^{-1/2} \qquad (2)$$

For $W/H \leq 1$,

$$Z_0 = \frac{60}{\sqrt{\epsilon_{eff}}} \ln(8\ H/W_e + 0.25\ W_e/H) \qquad (3)$$

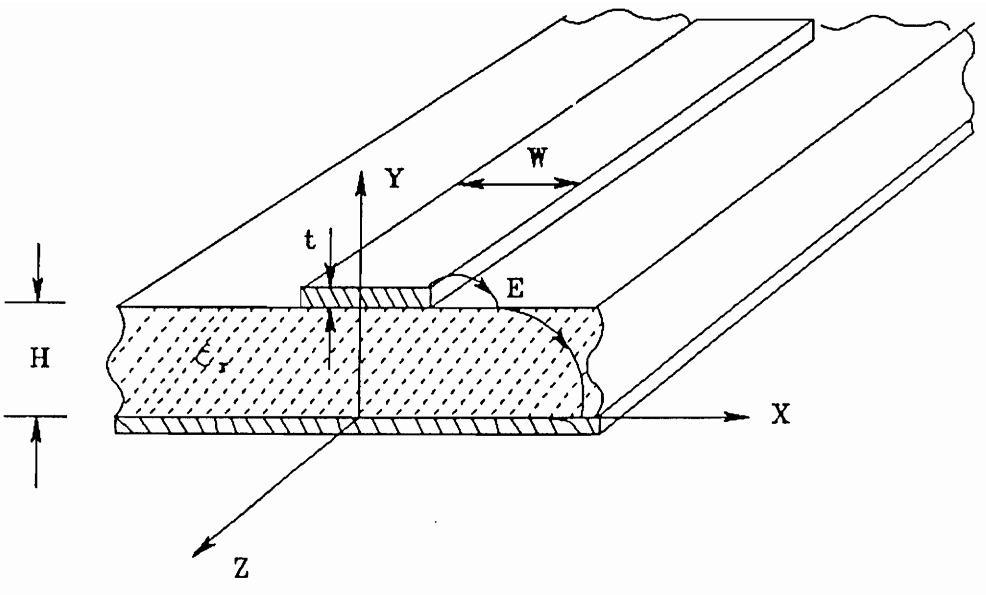

Figure 3.1 Microstrip Configuration

$$\epsilon_{eff} = \frac{\epsilon_r+1}{2} + \frac{\epsilon_r-1}{2}[(1+12H/W_e)^{-1/2}+0.04(1-W_e/H)^2] \quad (4)$$

where,

For $W/H \geq 1/2\pi$:

$$W_e/H = W/H + \frac{t}{\pi H}\left(1 + \ln\frac{2H}{t}\right) \quad (5)$$

For $W/H \leq 1/2\pi$,

$$W_e/H = W/H + \frac{t}{\pi H}\left(1 + \ln\frac{4\pi W}{t}\right) \quad (6)$$

3.2.2. Coplanar Transmission Line

A coplanar transmission line consists of three conducting strips; a central strip of width 'S', and two ground planes of width W_G on each side of the central strip, as shown in Figure 3.2. The conductor thickness is denoted by 't'. The distance between the central strip and the ground plane strip is designated by 'W', and the thickness of the dielectric layer is designated by 'h'. Similar to microstrip line, the mode propagation in CPW is not a pure TEM mode because a longitudinal component of the magnetic field exists. Under the quasi-static approximation, the characteristic impedance Z_0 is given by [17],

$$Z_0 = \frac{30\pi}{\sqrt{\epsilon_{eff}}} \frac{K'(k)}{K(k)} \quad (7)$$

where

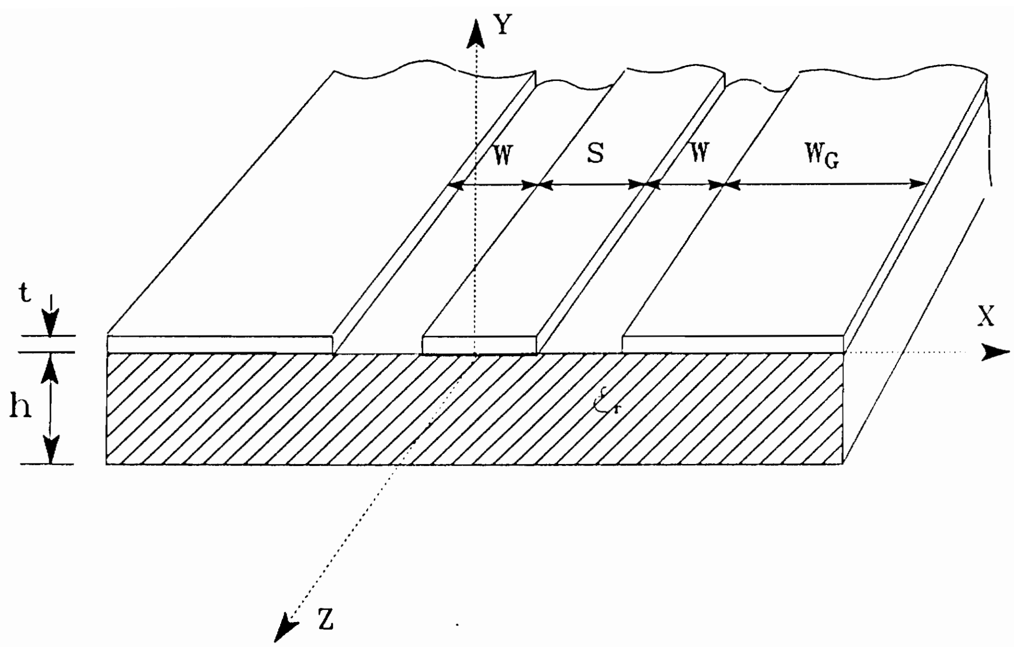

Figure 3.2 Coplanar Line Configuration

$$k = \frac{S}{S + 2W} \tag{8}$$

$$\frac{K'(k)}{K(k)} = \frac{1}{\pi} \ln \left[2 \frac{1 + \sqrt{k}}{1 - \sqrt{k}} \right] \quad \text{for } 0.707 \le k \le 1 \tag{9}$$

$$\frac{K'(k)}{K(k)} = \frac{\pi}{\ln \left[2 \frac{1 + \sqrt{k}}{1 - \sqrt{k}} \right]} \quad \text{for } 0 \le k \le 0.707 \tag{10}$$

$$\epsilon_{eff} = \frac{\epsilon_r + 1}{2} \left[\tanh\{1.785 \log(h/W) + 1.75\} + \frac{kW}{h} \{0.04 - 0.7k + 0.01(1 - 0.1\epsilon_r)(0.25 + k)\} \right] \tag{11}$$

3.3. Design Considerations

3.3.1. Power Splitter Design

It is assumed that baluns are designed to match to 50 Ω impedance level, which is the common impedance for most measurements and microwave systems. In order to ensure a balun to have a 50 Ω input and two 50 Ω outputs, a matching network, which is also a power splitter, is needed. Ideally, the input signal is equally split into two outputs. The phase of one of the outputs is converted by 180 degrees. With respect to input, each output is decreased by 6 dB. Considering effects of reflection from any output side, three identical resistors R's are selected to construct the splitter, as shown in Figure 3.3. The

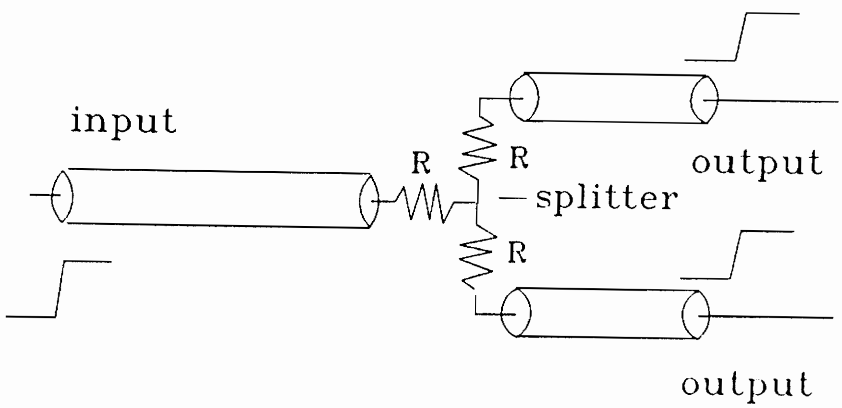

Figure 3.3 Power Splitter Configuration

condition of matching between the input and the splitter requires R_{in} to be equal to 50 Ω. Then, the value of the resistor R can be determined by:

$$R_{in} = 50 = \frac{50 + R}{2} + R \qquad (12)$$

Solving for R yields a numerical value equals to 16.67 Ω.

3.3.2. Coplanar Line Balun and Microstrip Line Balun

A computer package called LineCalc[18] was used to help design both a coplanar line and a microstrip line. The package is specially designed for studying the relationship between the electrical and physical parameters of transmission lines.

1. Coplanar balun design

The layout of the coplanar line balun is illustrated in Figure 3.4. The line is to be realized on ROGERS RT/duroid 6010.2 Teflon-Ceramic composite substrate, which has a relative dielectric constant of 9.8 and is 25 mils thickness. The conductor material is copper cladded to the substrate that has a thickness of 1.4 mils. Based on these material parameters and the requirement of 50 Ω characteristic impedance, LineCalc results in the dimensions of the coplanar line as follows:

Width of the signal line: S = 26 mils

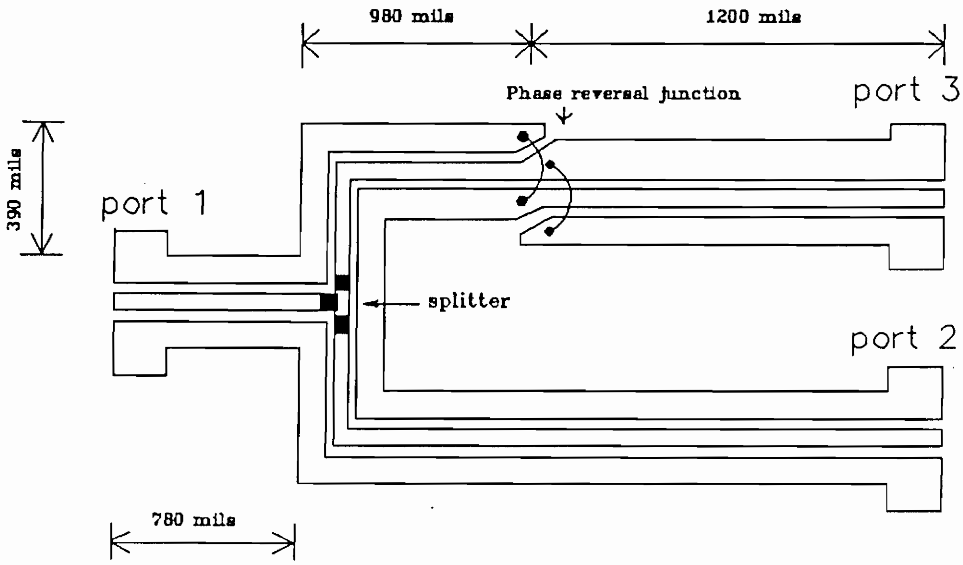

Figure 3.4 Coplanar Line Balun

Gap: $W = 10$ mils

Width of the ground plane: $W_G = 50$ mils

Effective dielectric constant: $\epsilon_{re} = 4.87$

The phase reversal junction is realized by exchanging the signal conductor and the ground conductor. Two wire-jumpers are used to make the exchange. The shape of the jumpers may affect the quality of the junction and should be adjusted to obtain the best performance.

2. Microstrip balun design

For the microstrip line, the layout is designed as shown in Figure 3.5. The line is realized on ROGERS RT/duroid 6010.2 Teflon-Ceramic composite substrate with 9.8 dielectric constant and 25 mils thickness. For the 50 Ω characteristic impedance, the dimensions of the microstrip line are given by LineCalc as follows:

Width of the signal conductor: $W = 22$ mils

Width of the ground conductor: $W_G = 222$ mils

Effective dielectric constant: $\epsilon_{re} = 6.6$

Unlike in the coplanar line, no jumpers are needed to realize the phase reversal junction. It is made through changing the dimensions of the signal conductor and the ground conductor. For a smooth transition, the width of the signal conductor gradually changes from 22 mils to 222 mils while the ground conductor changes from 222 mils to 22 mils at the junction. The degree of the smoothness is to be experimentally optimized at a later time.

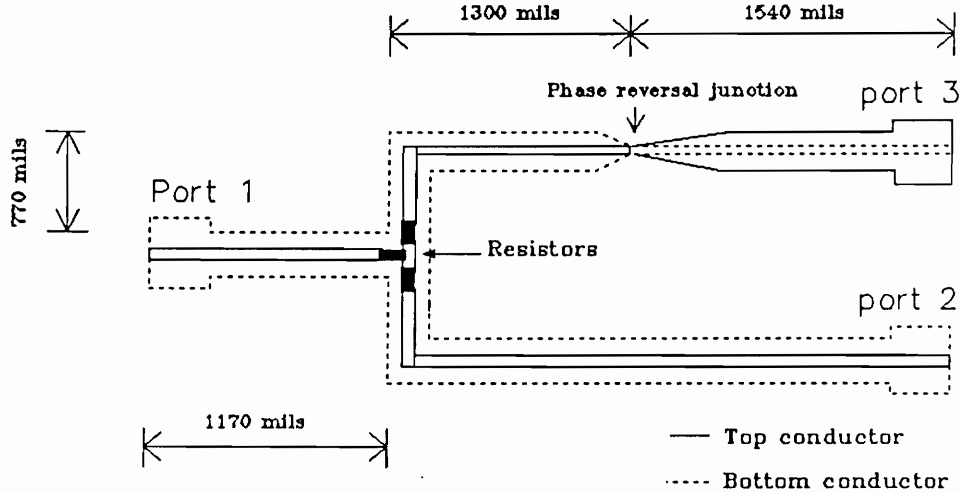

Figure 3.5 Microstrip Line Balun

3.4. Fabrication Process

The process of fabrication involves two major aspects: selecting resistors for the splitter and chemical etching of double-sided copper-cladded Teflon-ceramic composite board.

The chemical etching process involves several steps. The double-sided copper-cladded Teflon-ceramic composite board is cut into the desired size 3" x 4". Then photoresist is coated uniformly on both sides of the board by a high speed spinner. The photo coating is exposed to ultraviolet light source through the image negative for a certain period of time. The exposed photoresist is washed off in water. The remaining photo resist is then baked at 100° C for 10 minutes in order to be hardened. Finally, the board is etched by emerging it into the copper etchant until the copper that is uncovered by the photoresist is completely etched off. A good line definition is achieved by accurately controlling the etching time.

As seen later, the bandwidth of the splitter, or the resistors, sets limitation to high frequency performance of the balun. In other words, the higher the bandwidth of the splitter, the higher the cutoff frequency of the balun. The resistors of the splitter can be printed using the thick film technology. Then the printed resistors are trimmed to accurate value 16.67 Ω. Since the printed resistors cannot be used on the Teflon-ceramic composite substrate, commercial chip resistors, size 20 x 30 $mils^2$, have to be used. A problem encountered when using the chip resistors is that it is difficult to have uncommon value 16.67 Ω.

Therefore, three 50 Ω chip resistors are stacked up to achieve 16.67 Ω. The process requires careful soldering technique in order to achieve good results.

3.5. Conclusion

In order to match a balun to 50 Ω to both the input and the outputs, three 16.67 Ω chip resistors are used to realize a splitter, which is also a 6 dB power splitter for the balanced outputs. The wire jumpers are used at the phase reversal junction on the coplanar line balun to exchange the signal conductor and the ground conductor. The phase reversal junction on the microstrip line balun is realized by gradually changing the dimensions of the signal conductor and the ground conductor. The baluns are realized through the chemical etching process.

CHAPTER IV

MEASUREMENT IN TIME AND FREQUENCY DOMAINS

4.1. Introduction

Time domain measurement techniques have been widely used for determining reflection and transmission of microwave devices. Through the information from the reflection and transmission, the devices can be characterized and modeled. In frequency domain, S-parameters and bandwidth of the device under test can be determined using a network analyzer. The state-of-art of time domain measurement instrument and frequency domain measurement instrument are used to measure the wideband baluns.

4.2. Principles of Time Domain Measurement Techniques[19]

Time domain measurement techniques include Time Domain Reflection (TDR) and Time Domain Transmission (TDT) techniques. The time domain techniques are based on the following principle. A step pulse (or a impulse) produced by the pulse generator is launched into the device under test (DUT). Part of the pulse is reflected when it encounters a discontinuity while the rest of the pulse is transmitted through the device. Useful information about the DUT is contained in the reflected and transmitted waveforms.

4.2.1 TDR measurement techniques

Figure 4.1 shows a TDR setup, which is generally used for time domain measurements. The setup consists of three main parts: a fast transition pulse generator, a feed-through sampler, and a sampling oscilloscope. The sampler is interfaced to the scope by a microcomputer. The reflected signal can be evaluated by a reflection coefficient ρ and the traveling distance ℓ, which are given by

$$\rho = \frac{V_{reflected}}{V_{incident}} \qquad (13)$$

and

$$\ell = t_t \frac{v_{effective}}{2} \qquad (14)$$

where $V_{reflected}$ and $V_{incident}$ are the reflected voltage and incident voltage, respectively. $v_{effective}$ and t_t are the relative wave propagating velocity and traveling time, respectively. The reflected waveforms are picked up by the sampler and then displayed on the oscilloscope. The shapes of the waveforms are associated with various types of discontinuities, which include open circuit, short circuit, and impedance mismatch.

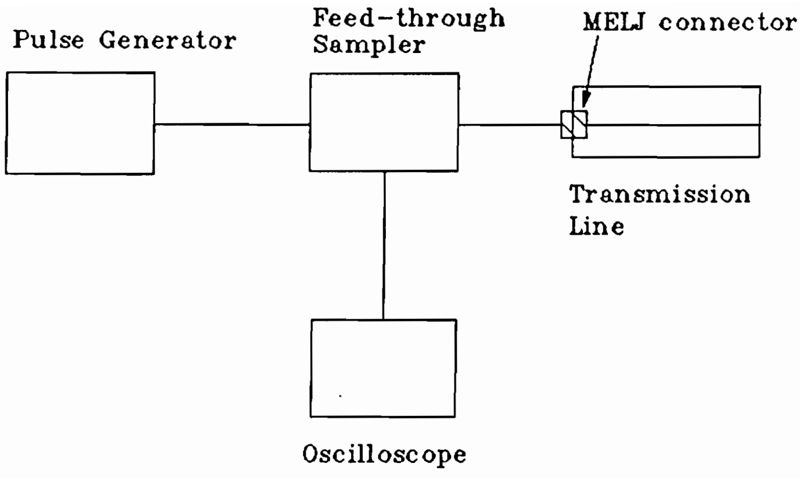

Figure 4.1 TDR Testing Setup

The TDR response of an open circuit is the same as the incident waveform, a reflection coefficient equals to +1. This is because no current can flow at the open node so that the whole pulse has to travel back, assuming no loss through the traveling path. The TDR response of a short circuit is the negative of the incident waveform, indicating a reflection coefficient equal to -1. This is due to the requirement of zero voltage at the shorted node so that a negative pulse has to travel back to negate the voltage at the node. The responses for the open circuit and short circuit are shown in Figure 4.2. The response of an impedance mismatch is in between that of the short and that of the open.

The reflection coefficients of reactive devices are functions of time, thus distorting the reflected waveform. The TDR responses of a capacitor C and an inductor L associated with a resistor R=50 Ω are also shown in Figure 4.2. When the step pulse hits the capacitor, the capacitor passes the current, acting as a short. As the capacitor is charged up, it starts to block the current, behaving like an open. For an inductor, its reaction to the step is to resist the rapid change of the fast transition. As shown, the responses of the reactive devices are characterized by the exponential curves. An exponential time constant T is used to describe the characteristics. T is given by [20],

$$T = C \frac{RZ_0}{R + Z_0} \quad \text{, for a shunt capacitor} \qquad (15)$$

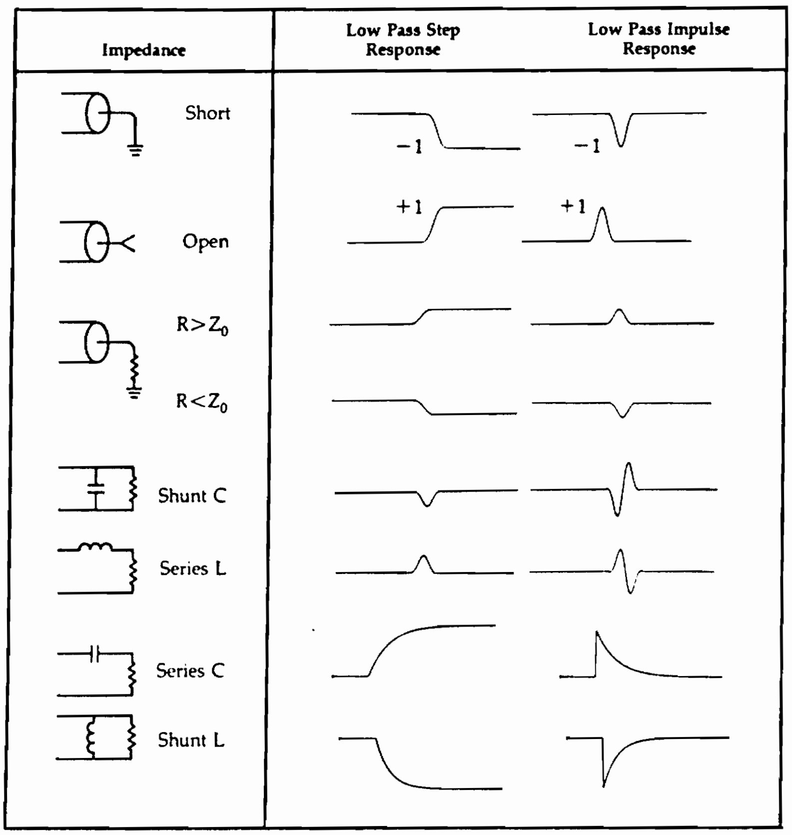

Figure 4.2 Characteristic Responses of Lump Elements

$$T = \frac{L}{R + Z_0} \quad \text{, for a series inductor} \qquad (16)$$

$$T = C\,(R + Z_0) \quad \text{, for a series capacitor} \qquad (17)$$

$$T = L\,\frac{R + Z_0}{RZ_0} \quad \text{, for a shunt inductor} \qquad (18)$$

where Z_0 is the characteristic impedance of a transmission line. The time constant T is easily determined by the time at the half voltage point of the exponential curve by $T = t/0.69$, where t is the time at the half voltage point. The above mentioned equations can be used to evaluate unknown values of the reactive devices from the response waveforms. Note that the reactance also slows down the rise time of the pulse.

4.2.2 TDT measurement techniques

Figure 4.3 shows the TDT setup. The setup is different from that of TDR in that the sampler and the oscilloscope are connected to end of the device under test. The transmission is evaluated by a transmission coefficient τ, which is given by,

$$\tau = \frac{V_{transmitted}}{V_{incident}} \qquad (19)$$

where $V_{transmitted}$ is the transmitted voltage. Another parameter used for describing the transmission is the delay T_t, which is related to the transmission path length by

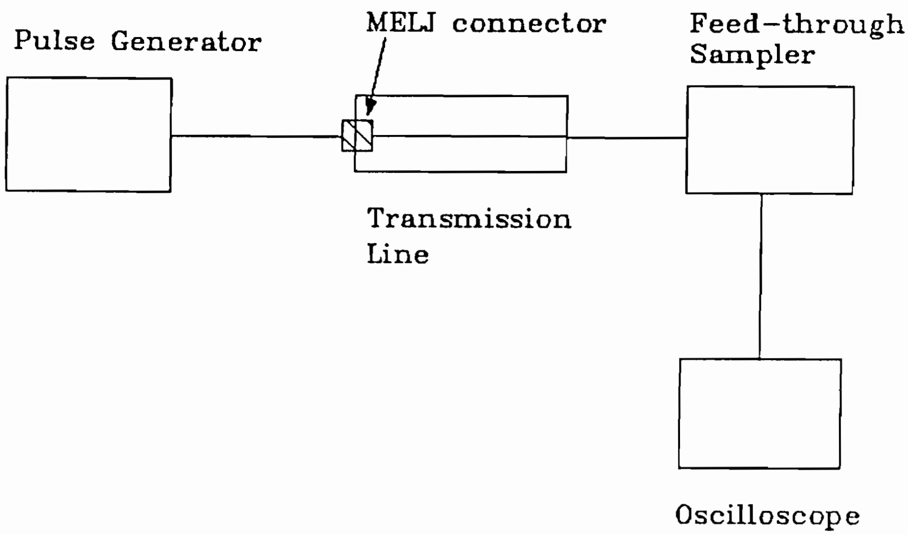

Figure 4.3 TDT Measurement Setup

$$T_t \cdot v_{effective} = \text{path length} \tag{20}$$

The responses in transmission are similar to those in reflection. It is easy to see that the relation between the reflection and the transmission is given by,

$$\tau = \rho + 1 \tag{21}$$

According to the description of reflection and transmission, it can be recognized that time domain measurements can determine types of devices and their electrical parameters by examining the reflection and transmission waveforms. The great advantage to work in time domain is that problems are worked in the real world, where one can get a clear insight into the problems. This advantage will be demonstrated through the work.

4.3. Principles of Frequency Domain Measurement Techniques[19]

In order to determine reflection and transmission of a microwave signal, or energy, through a device in frequency domain, a set of scattering parameters, known as S-parameters, are defined in terms of incident voltage waves and reflected voltage waves. For a two-port network shown in Figure 4.4, S-parameter is described as follows,

$$V_{1r} = S_{11} V_{1i} + S_{12} V_{2i} \tag{22}$$

$$V_{2r} = S_{21} V_{1i} + S_{22} V_{2i} \tag{23}$$

where V_{1i} and V_{2i} are the incident voltage waves at port 1 and

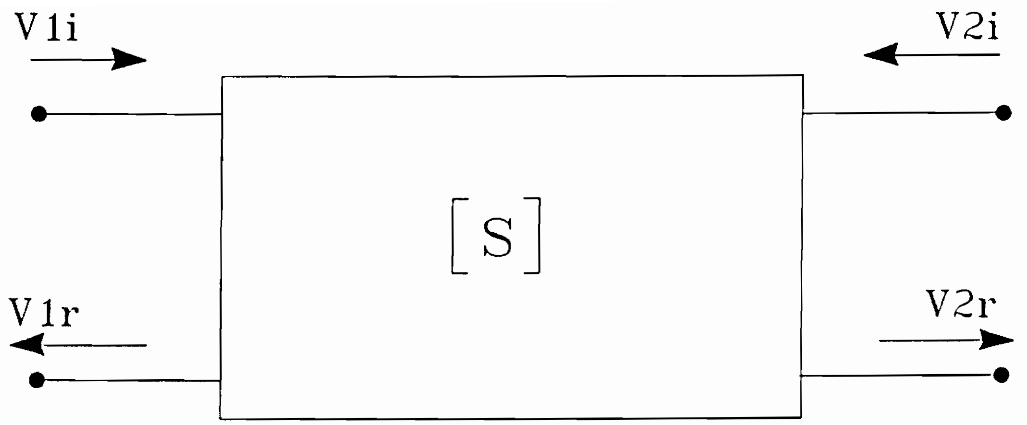

Figure 4.4 Two-Port Network Representation

port 2, respectively, and V_{1r} and V_{2r} are the reflected voltage waves at port-1 and port-2, respectively. S_{11} is the reflection coefficient at port-1, S_{21} is the transmission coefficient from port-1 to port-2 of the network, S_{22} is the reflection coefficient at port-2, and S_{12} is the transmission coefficient from port-2 to port-1.

Measurements of S-parameter are generally accomplished by a network analyzer system. The system consists of a signal source, an S-parameter test set, a network analyzer, and a display unit. The setup of the frequency domain measurement using a HP 8510B Network Analyzer is shown in Figure 4.5. In evaluating S_{11}, the test set uses a dual directional coupler connected as a reflectrometer, while in measuring S_{21}, it essentially acts as a power divider. Two outputs from the test set are a reference signal and either a reflected signal or a transmitted signal, containing information about S_{11} or S_{21}, respectively. These signals are measured in the complex ratio measuring unit, which is built in the network analyzer. The results from the unit are obtained in terms of the magnitude and phase of S_{11} or S_{21}. Furthermore, they can be sent to the display unit for displaying or to a computer for processing.

The measurement accuracy is the main concern in measuring S-parameters using a network analyzer system. This is because imperfections in the measuring system hardware introduce significant errors. These errors can be corrected by a calibration procedure, where standard terminations such as match, short and open are connected to the system to eliminate the errors.

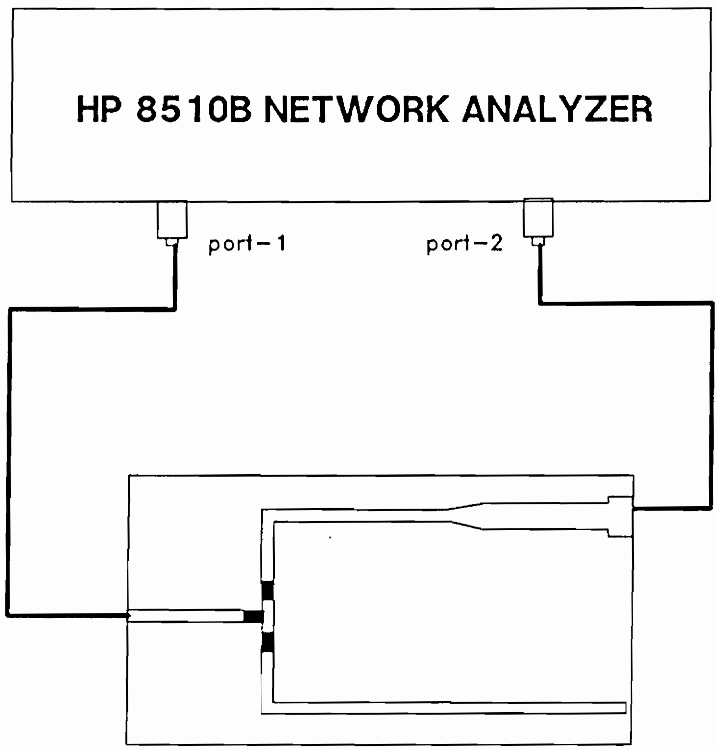

Figure 4.5 Frequency Domain Measurement Setup

4.4 Time Domain Measurements of Baluns

The baluns to be measured by time domain techniques are the coplanar line balun and the microstrip line balun. The instrument used for the measurement is HP-85121 digital oscilloscope and HP-85122 pulse generator, which provides a step pulse with a magnitude of 400 mv and rise time of 30 ps.

4.4.1. Coplanar Line Balun Measurement

In order to characterize and optimize the performance of the coplanar line balun, both TDR and TDT measurements are to be conducted. The balun is labeled as a three-port device. Port1 is designated for the input terminal, while port2 and port3 for non-reversal output and reversal output, respectively. SMA Modified End Launch Jack connectors (MELJ) are used for transition from the testing cable to the planar transmission line on the balun. TDR waveform is observed at the port1, shown in Figure 4.6. TDT waveforms are observed port2 and port3. For comparison, TDT waveforms are displayed at the same window on the scope, shown in Figure 4.7. As seen from the time domain waveforms measured, they are severely distorted.

Based on the time delays calculated, it becomes easy to locate the sources of the waveform distortions. Analyzing the TDR waveform, the first dip, appearing as capacitive response, is caused by the transition of the connector. The response at the splitter position, after t = 147 ps is fairly complicated due to the combination of R, L, and C. Phase reversal junction causes a drop in impedance after t= 257 ps from the splitter. In the TDT waveforms, one important observation is that after 220 ps, two output curves start to decay. This

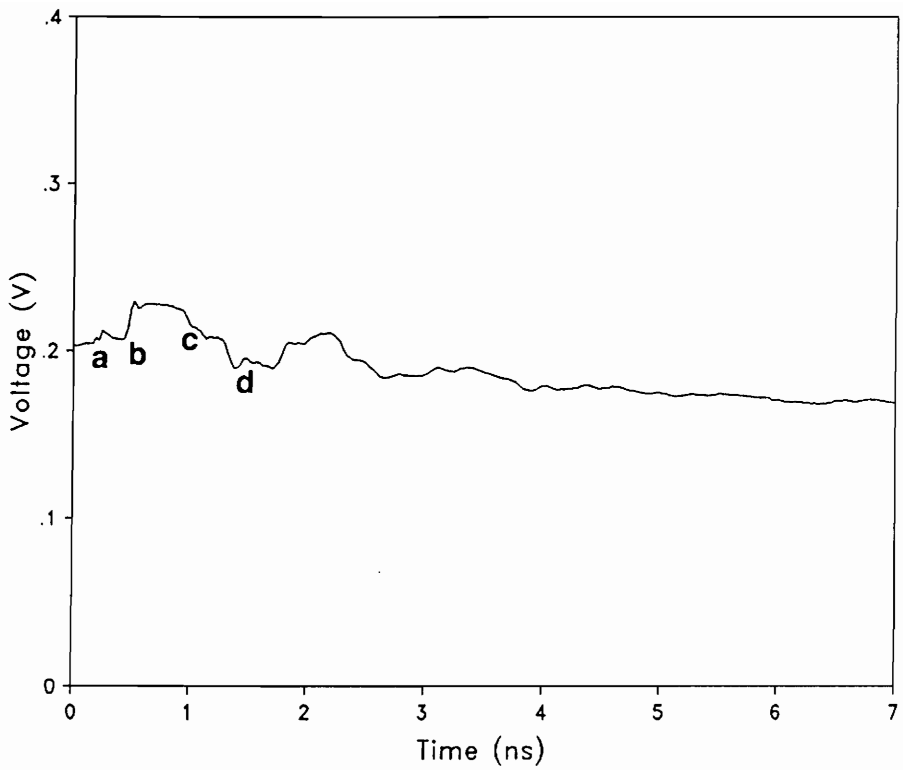

a __ Input connector
b __ Splitter
c __ Reversal junction
d __ Output connector

Figure 4.6 TDR Waveform of the Coplanar line Balun

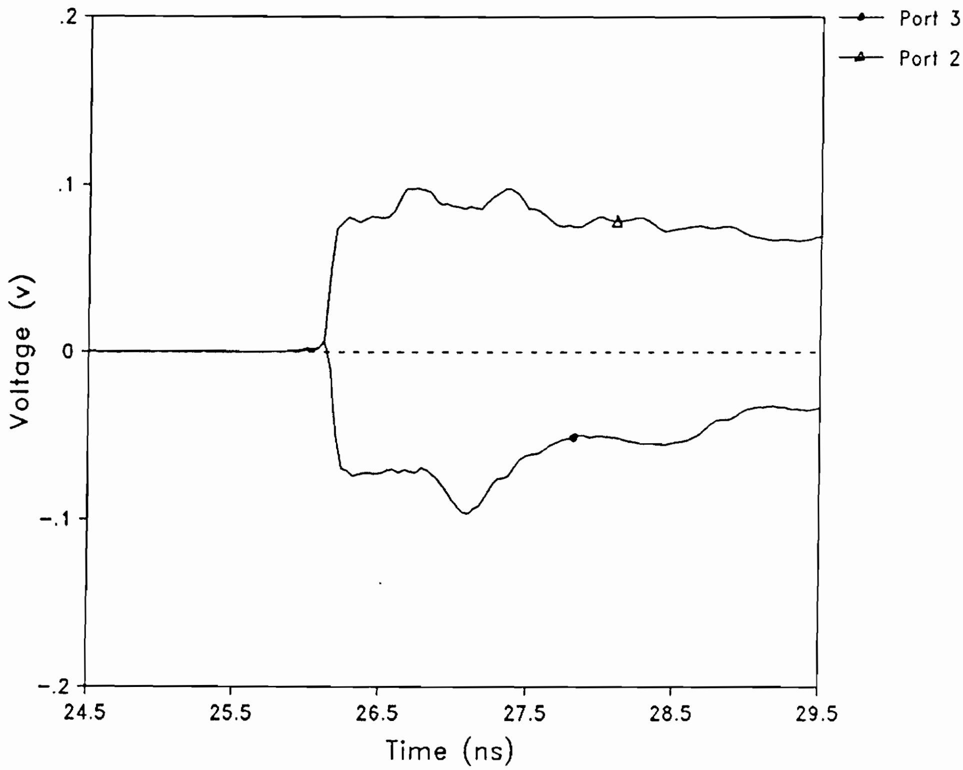

Figure 4.7 TDT Waveforms of The Coplanar Line Balun

is due to a short, caused by the phase reverse, through the common ground. This phenomenon will be discussed in more detail in the next chapter.

4.4.2. Microstrip Line Balun Measurement

The same measurement procedure as in the coplanar balun is used to measure the microstrip line balun. TDR and TDT waveforms are shown in Figure 4.8 and Figure 4.9, respectively. There is no significant reflection apparent in the TDR waveform. The TDT outputs behave to be fairly balanced up to a duration of 7 ns. This duration corresponds to the length between reversal junction and the end of the 3-foot testing cable. It is not surprised that the waveforms are much better than those of the coplanar balun because of different field distribution between the two kinds of lines. In the coplanar line, half of the field coupling between the signal conductor and the ground conductor is through the air while another half of the coupling is through the substrate. In the microstrip line, most of the field coupling is through the substrate except a small amount of leakage. These are shown in Figure 4.10, and Figure 4.11, respectively. As a result, the field distribution in the coplanar line is much easier to be distorted than that in the microstrip line. It is more convinced to compare the distortion at the splitter. The chip resistors are mounted on top of the signal conductor. The field distribution in the coplanar line is changed significantly by the resistors while that in the microstrip line is negligible small. Another noticeable difference is the way to realize the phase reversal junction. For the coplanar line balun, the wire jumpers change the field distribution, causing the distortion of the waveform. For the microstrip line balun, the phase reversal junction is realized by the gradual variation of the line widths of both

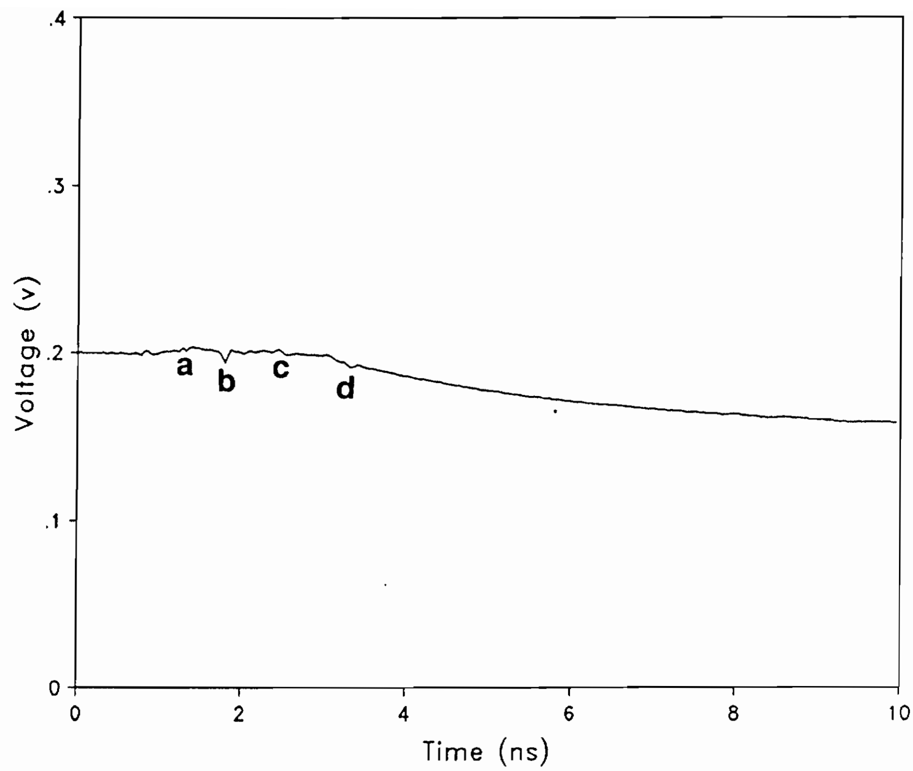

a __ Input connector
b __ Splitter
c __ Reversal junction
d __ Output connector

Figure 4.8 TDR Waveform of The Microstrip Balun

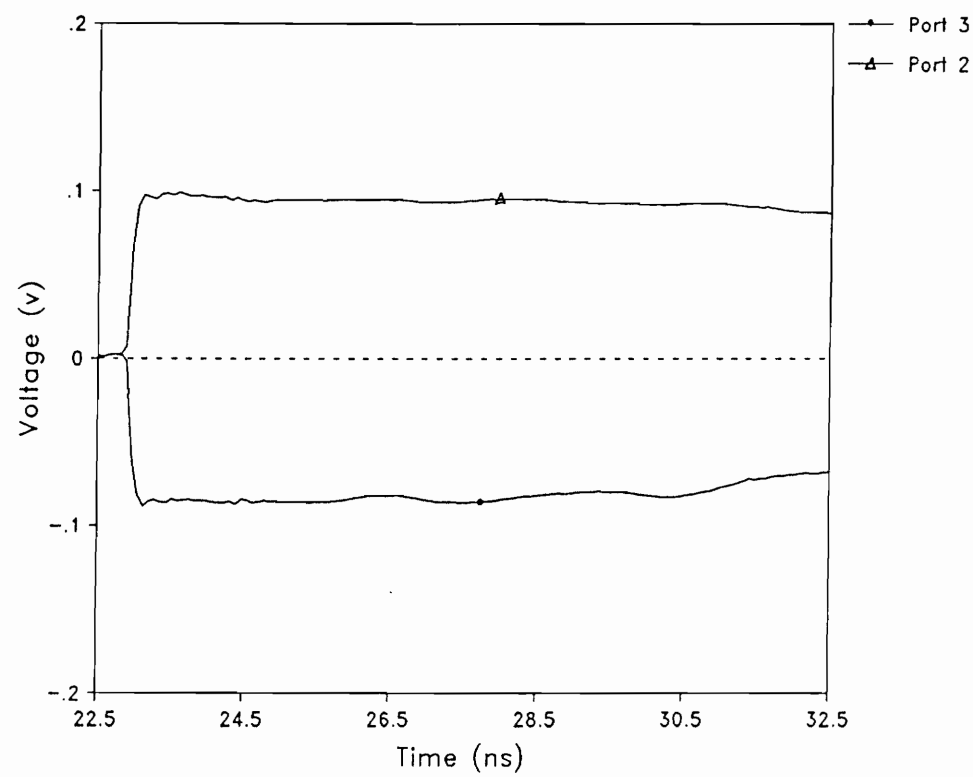

Figure 4.9 TDT Waveforms of The Microstrip Balun

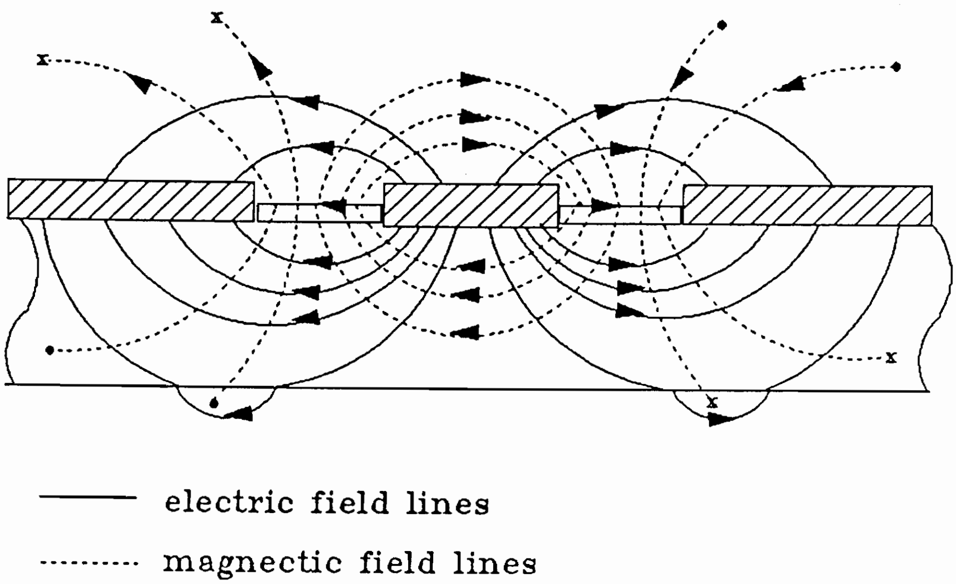

Figure 4.10 Electric and Magnetic Field Distributions in Coplanar Line Configuration

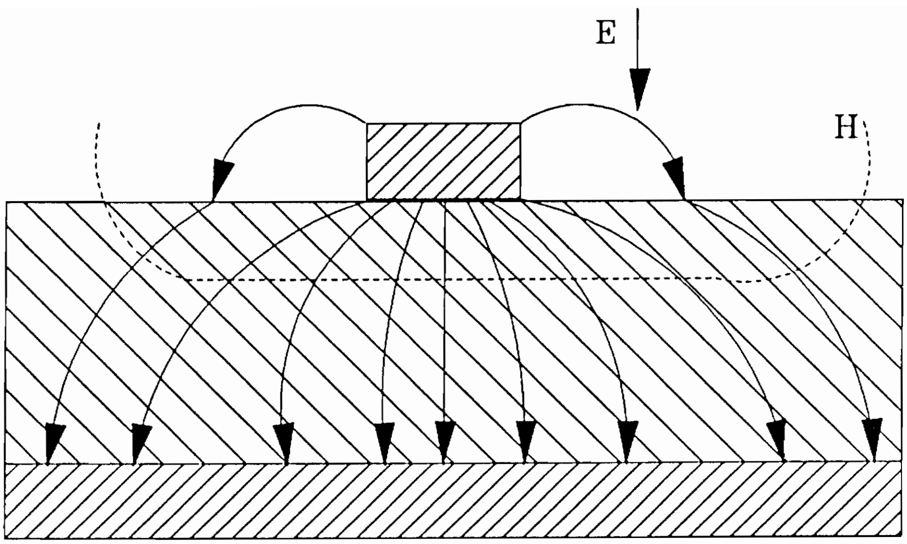

Figure 4.11 Electric and Magnetic Field Distributions in Microstrip Line Configuration

conductors. Therefore, no significant distortion of the field distribution occurs.

4.5. Frequency Domain Measurement

The results of the time domain measurements indicate that the microstrip line balun has much better performance than the coplanar line balun. Therefore, frequency measurement is conducted only on the microstrip line balun. The instrument used for the measurement is HP-8510 Network Analyzer, which has a sweeping frequency range from 45 MHz to 40 GHz. Before the measurement takes place, calibration is necessary to ensure measuring accuracy. The full two-port calibration is done in order to measure S-parameters of the three-port device, the microstrip line balun. The calibrated frequency range is from 45 MHz to 10 GHz. S_{11} and S_{21} are measured with a matched termination of port3 while S_{31} is measured with a matched port2. The measurement results are shown in Figure 4.12 for S_{11} and Figure 4.13 for S_{21} and S_{31}. From these figures, the 3 dB bandwidth of the balun is found to be of the order of 5 GHz which is the highest frequency of the MELJ connectors. The lower cutoff frequency is less than 45 MHz which is the lowest frequency possible with the measuring instrument. Within this frequency range, S_{11} is below -20 dB.

4.6. Conclusion

The principle of TDR and TDT techniques in time domain measurement is introduced. The principle is based on information about reflection and transmission to analyze the discontinuities, which affect the device's microwave

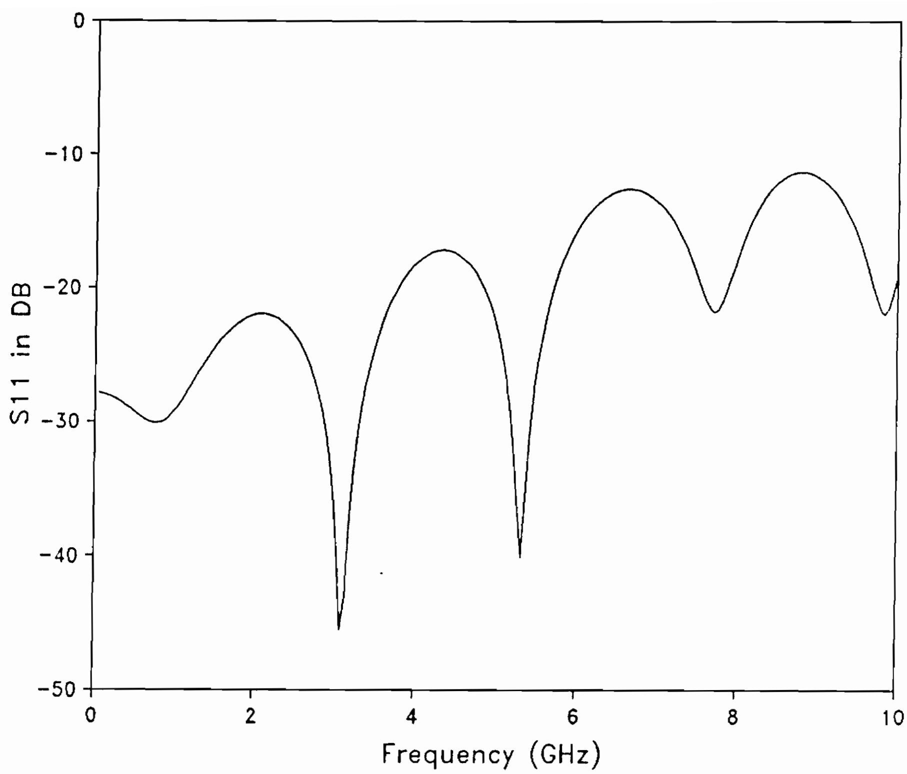

Figure 4.12 S11 of The Microstrip Balun

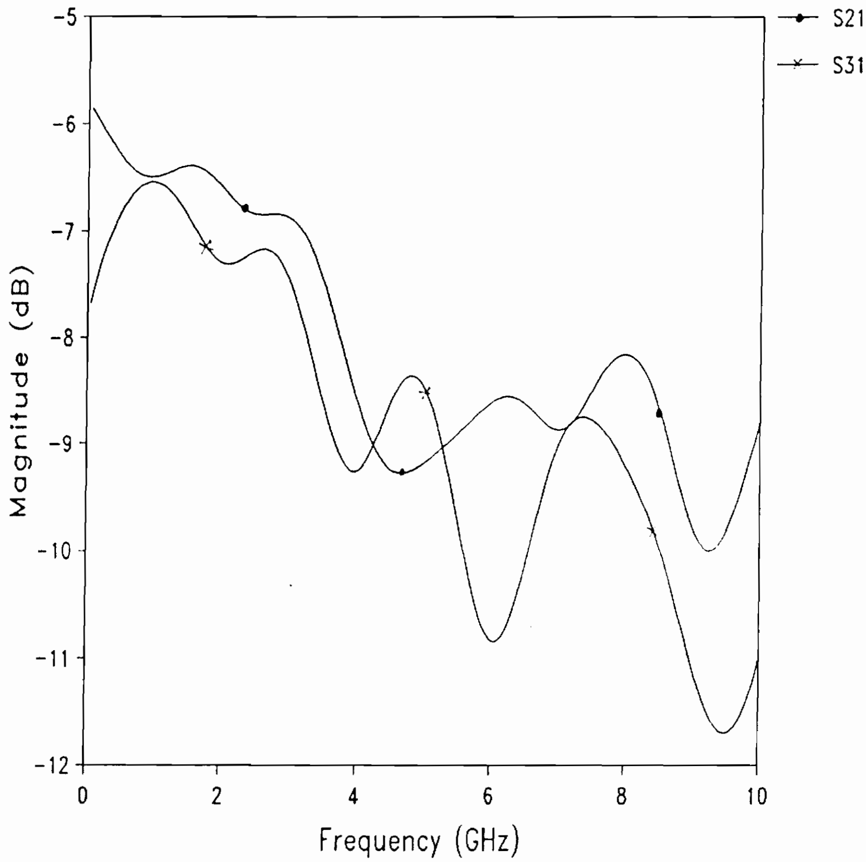

Figure 4.13 S21 and S31 of the Microstrip Balun

performance. The time domain measurements on both coplanar line balun and microstrip line balun are conducted. The results indicate that the microstrip line balun has better performance over the coplanar line balun mainly due to a smooth transition at the phase reversal junction in microstrip line balun. The high cutoff frequency performance is limited by the respective bandwidths of the power splitter, the coaxial to microstrip line connectors, and the transmission line itself. The low cutoff frequency performance is determined by the standing waves generated by the propagation of the ground currents as a result of the phase reverse. The time domain results also show various lumped circuit effects and their locations associated with the discontinuities. The frequency domain measurements is made only on the microstrip line balun, indicating a 3-dB bandwidth of the order of 5 GHz, which is the highest frequency of the MELJ connectors. The lower cutoff frequency is less than 45 MHz which is the lowest frequency possible with the measuring instrument.

CHAPTER V

MODELING AND CHARACTERIZATION OF WIDEBAND BALUNS

5.1. Introduction

Time domain techniques have been used to characterize and model microwave components, particularly those fabricated using hybrid technology. The models of these microwave components are usually represented by lumped circuit elements, which can be built in a computer package designed for microwave circuit design. The technique consists basically of comparison of a device measured response with a simulation response of a constructed network model in time domain. The comparison is accomplished by a computer package called Modified Transient Circuit Analysis Package (MTCAP)[21]. The models obtained in the time domain can be also verified in the frequency domain by comparing the S-parameters of the network models, simulated by PSpice, with the measured S-parameters resulting from the Network Analyzer measurements. These techniques are to be applied to modeling and characterization of the microstrip line balun.

In this chapter the time domain techniques in modeling and characterization microwave components are described. Then, the procedure for modeling and characterization of the microstrip line balun is thoroughly presented, based on physical analysis of the balun. Finally, a model is illustrated for the balun and some discussions are to be carried out.

5.2. Time Domain Modeling Techniques[22]

The time domain modeling technique involves three basic steps. First, two TDR waveforms are acquired using the measurement technique described in the previous chapter. The first TDR waveform is the reflected waveform from the device to be modeled, and the second waveform is the reference waveform which is obtained by replacing the device to be modeled with a standard short termination. Second, an initial model, represented by lumped circuit elements, are devised. The initial model is based on two aspects of knowledge; knowledge of the physical nature of the elements and the structure details of the device as well as knowledge of time domain behaviors of various lumped circuit elements, as described in the previous chapter. Third, simulation of the initial model is carried out using MTCAP. Comparison of the simulated waveform with the measured TDR waveform is performed in an iterative manner. Values of the elements in the model are correspondingly modified until the simulated waveform matches the measured TDR waveform.

The process is started with the acquirement of the TDR waveforms. It is of crucial importance to acquire the reference waveform right at the position of the device to be modeled since the reference waveform is used to excite the network model during the simulation. Problems usually arise in acquiring the reference waveform, namely; 1) the position cannot be located exactly and 2) a standard short cannot be connected so that an approximate short has to be used. For the former case, an extra time delay or advance is introduced, leading to an inaccurate model and sometimes difficulties in the simulation by MTCAP. For the latter case, the approximate non-standard short introduces parasitic capacitive and/or inductive effects in the model.

During the MTCAP simulation, the values of the elements in the model are adjusted in an iterative manner to optimize the model. In this iterative process, each discontinuity is dealt with one at a time in the order of its physical location away from the launching port. Once an element value due to a discontinuity is optimized, any variation of element values related to later discontinuities is not expected to affect the simulated response waveform of previous times. This is a unique feature of performing the modeling process in the time domain. Once an acceptable match between the simulated waveform and the measured waveform is achieved, the model can be represented by an equivalent network.

5.3. Modeling and Characterization of Microstrip Line Balun.

A TDR response is characterized by dips, peaks, oscillations, and relaxations. These variations are recognized as reflections caused by distributed and/or lumped discontinuities on the transmission paths. These discontinuities can be modeled as one or more ideal components connected in shunt or in series with the transmission line. Chapter IV provides the response of various ideal components.

Examining the configuration of the balun, one can find that there are four locations causing discontinuities. These locations correspond to physically regions of the MELJ connectors, the 6-dB power splitter, the 90-degree bend, and the phase reversal junction. The following sections describe the way to model these discontinuity sources according to their physical natures.

1) MELJ connectors. An MELJ connector provides a transition from a coaxial cable to a planar transmission line. There are two consideration factors. One factor is concerned with the propagation mode in coaxial cable being basically pure TEM mode while that in a microstrip line is not. Therefore, the field is inevitable disturbed through the transition, resulting in a discontinuity, unless an ideal transition can be provided. Another factor is recognized as non–ideal electrical transition introduced by the soldering process, which is needed to connect the pin of the MELJ to the signal conductor of the microstrip line. Since the soldering operation is a sensible process highly dependent on the operator and the material involved, it leads to difficulty to achieve a consistent model of the transition. Usually, the connector with the transition is modeled as a combination of a delay transmission line, an inductor and/or a capacitor.

2) 6-dB power splitter. The structure consists of three 16.67 Ω commercial chip resistors, fabricated using thick film technology. It has been shown that at microwave frequencies, such a chip resistor used on a transmission line acts as a

combination of a resistor, a capacitor in parallel with the resistor, and two capacitors in shunt cross the transmission line. In addition, an inductor in series with the resistor can also be included, as shown in Figure 5.1. However, compared to the other parasitic components, the effect of the inductor is usually negligible. Considering a model of the chip resistor containing resistance and capacitance, one can understand the reason that the high cutoff frequency of the balun is partly limited by the splitter. The values of the parasitic capacitors vary with each specific chip resistor and the way it is connected to the transmission line.

3) 90-degree bend. A bend with an angle θ has been modeled [17]. The model shows that the bend can be represented by a combination of two inductors in series and a capacitor in shunt, as shown in Figure 5.2. These components are basically distributed components, introduced by the change of field distribution at the corner. Usually, a smooth bend has less disturbance than a sharp bend. The values of the distributed components are mainly determined by the bending angle. The effects of the inductors are negligible compared to the capacitance effect.

4) Phase reversal junction. Modeling of the phase reversal junction is an essential task in modeling the balun. This is because of complexity of the analysis of the field distribution around the junction. In order to understand the modeling process clearly, the modeling of the phase reversal junction is to be discussed in a separate section.

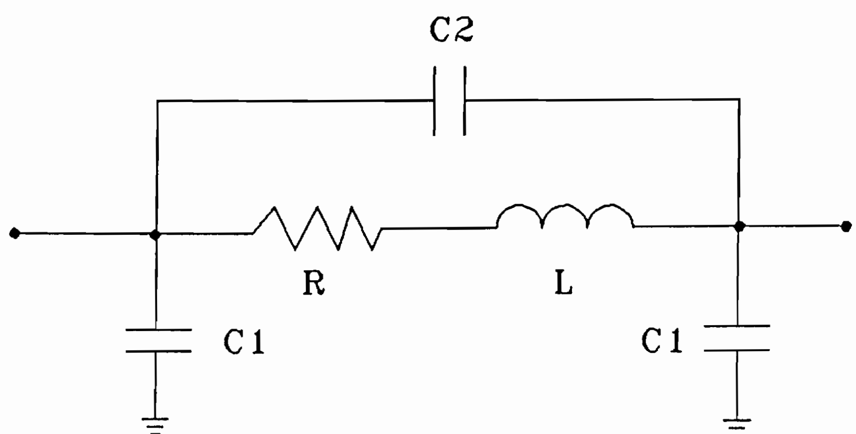

Figure 5.1 Chip Resistor Network Model

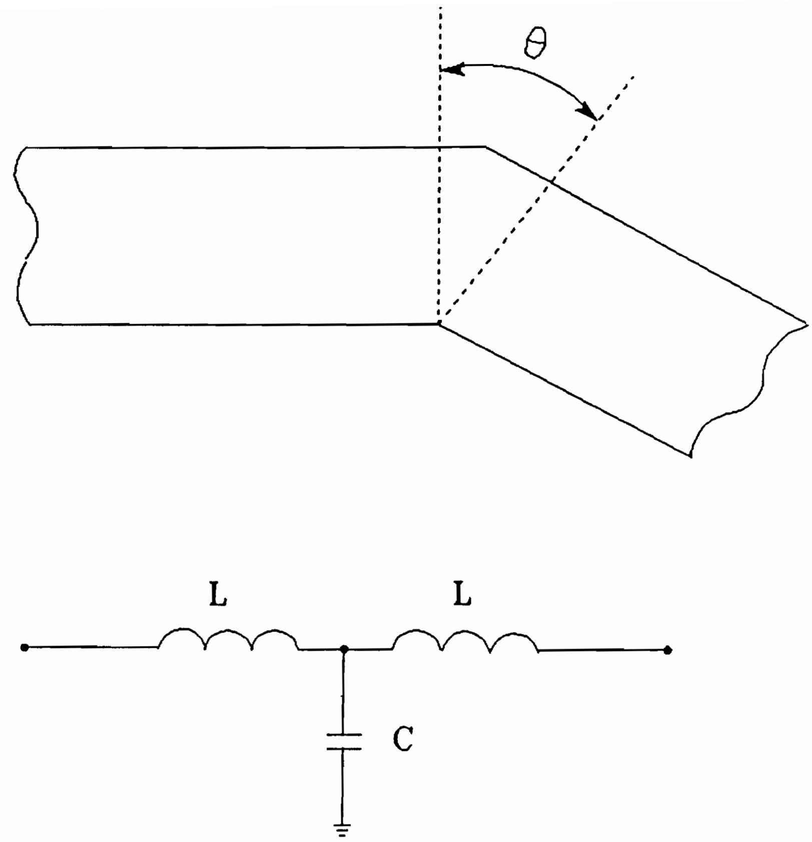

Figure 5.2 Microstrip Bend Network Model

5.4. Modeling of the Phase Reversal Junction

The modeling of the phase reversal junction starts by examining the TDR waveform taken at the input port and the TDT waveforms at the output ports. Two cases are considered in the process as follows:

Case 1: A step pulse is applied at the port-1. Port-2 and port-3 are connected through two extended cables to TDT sampling ports. The measurement setup is shown in Figure 5.3. The TDR and TDT waveforms are acquired. They are illustrated in Figure 5.4 and Figure 5.5, respectively. Note that two grounds of the output ports are actually connected to each other through the cables and then the TDT measuring system. Some interesting phenomena can be observed in these waveforms. At certain point of time, the curve of the TDR response starts to decay until a saturated value is reached. Before that point, a drop occurs, corresponding to a decrease in the characteristic impedance. In the TDT waveform, two balanced output signals are observed. After a period of time, the output signals start to decay. For the TDR measurement, the setup in Figure 5.3 is equivalent to Figure 5.6, where the extended cables, instead of being connected to the TDT sampling ports, are terminated with two 50 Ω matching terminations through which two grounds are also connected. Changing the length of the extended cable, one can find that the slope of the curve's decaying changes. The shorter the cables, the faster the curve decays. At the extreme case, the length of the extended cable is zero. The changes in the length of the extended cable lead to change in S-parameters at low frequency range in the frequency domain. In other words, the extension

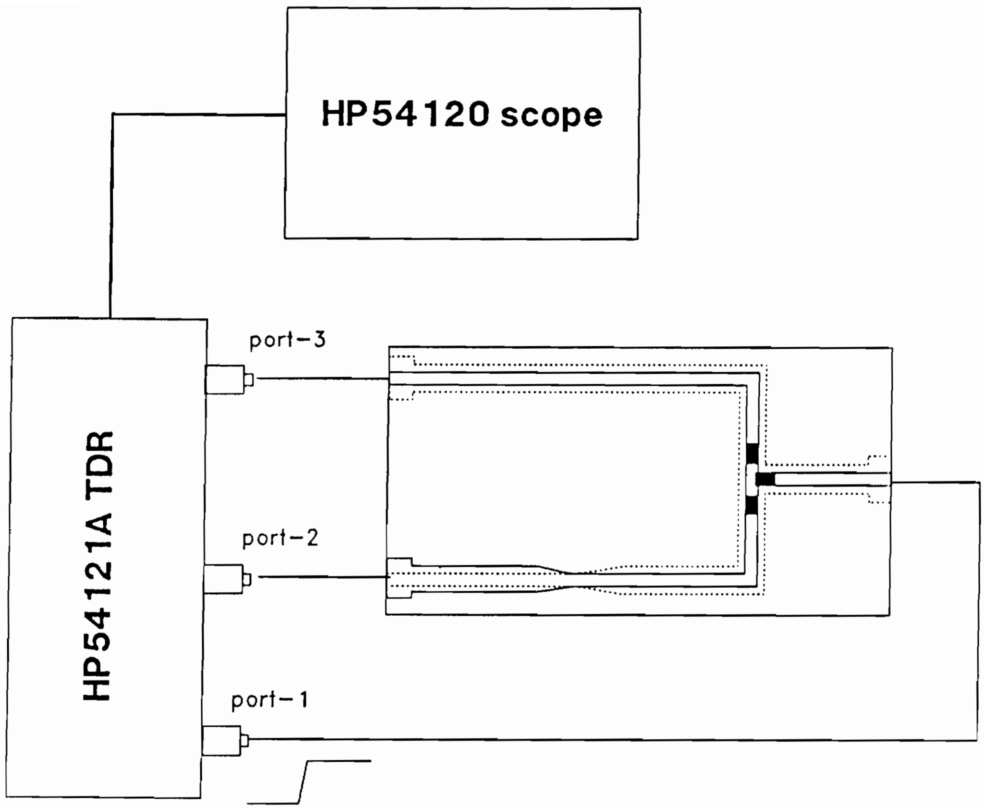

Figure 5.3 Time Domain Measurement Setup for Microstrip Balun

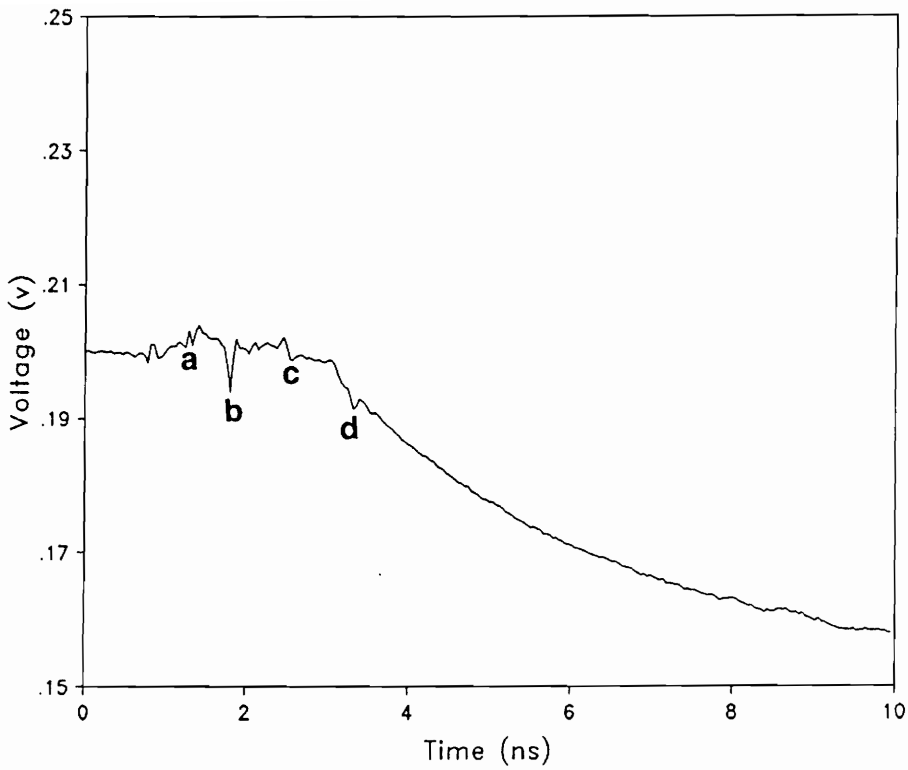

a __ Input connector
b __ Splitter
c __ Reversal junction
d __ Output connector

Figure 5.4 TDR Waveform of the Microstrip Balun

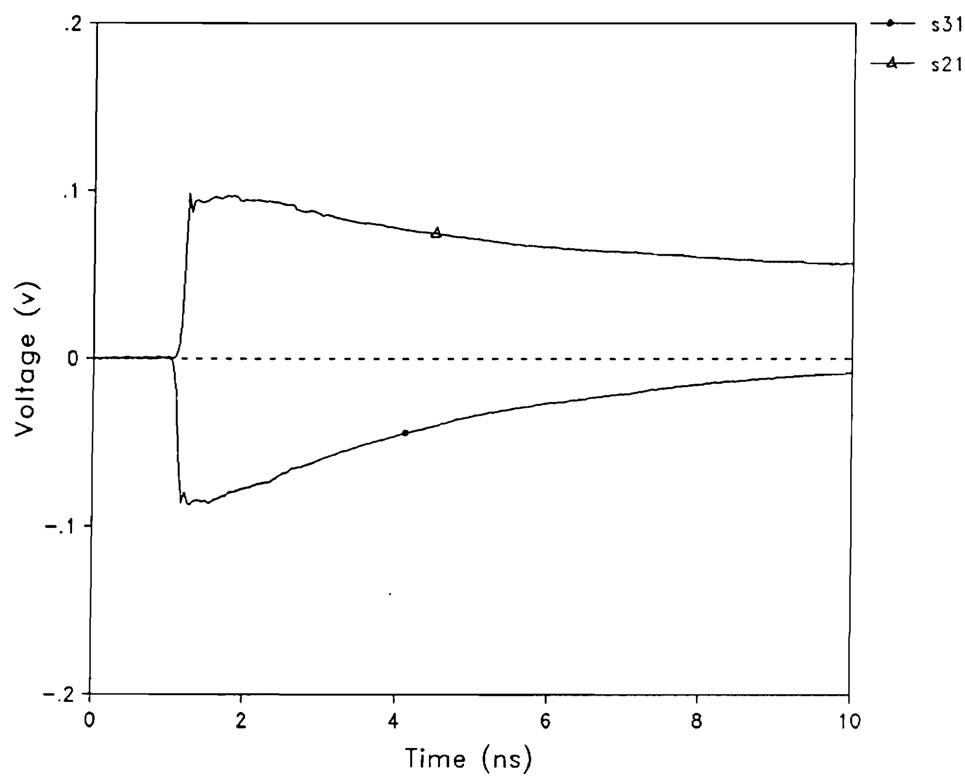

Figure 5.5 TDT Waveforms of the Microstrip Balun

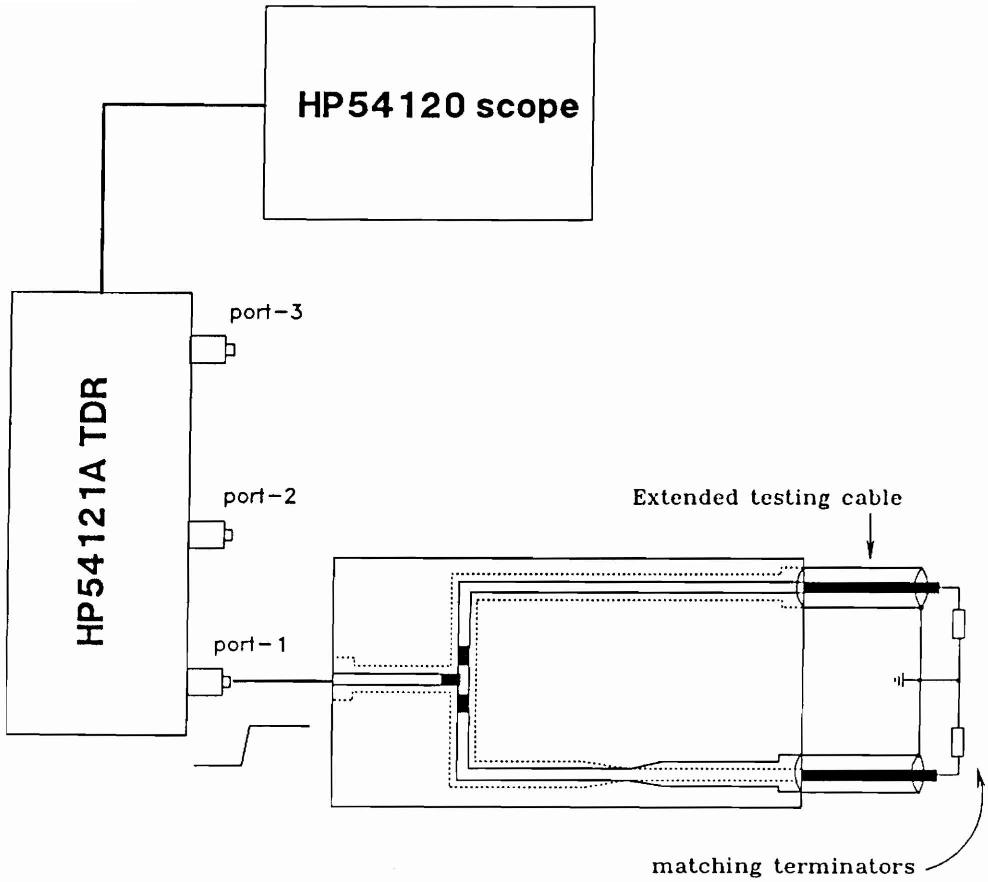

Figure 5.6 Equivalent Connection Diagram to Figure (5.3)

beyond the output ports affects only the low cutoff limit of the balun.

Case 2: with the extended cables attached to the output ports, two grounds are not connected to each other beyond the output ports. Instead of decaying as in case 1, the TDR response exhibits a damped oscillation, as shown in Figure 5.7. The frequency of the oscillation is related to the length of the cables. The longer the cables, the slower the oscillation.

In order to understand the phenomena occurred due to the phase reversal, it is necessary to analyze the physical nature of the process associated with the reversal junction. At the junction, the signal conductor and the ground conductor are exchanged. The exchange is realized by changing the geometries of the related conductors. A tapered-type transition is designed to have a smooth transition. In this transition region, the field is forced to reverse its polarity. The perturbation in this transition region leads to a leakage field which activitates other propagation modes.

Upon a careful observation of the balun's configuration, one can find that the two arms of the balun form a transmission media for the leakage fields. As expected, a transmission line formed in this way should exhibit a high impedance level. There exist two high impedance lines for propagation of the leakage fields. One line extends between the phase reversal junction to the output connector and beyond if the coaxial lines are attached to the output ports. And, the other line propagates the leakage fields from the phase reversal junction back to the 90-degree bend, where it terminates into the 50 Ω microstrip line.

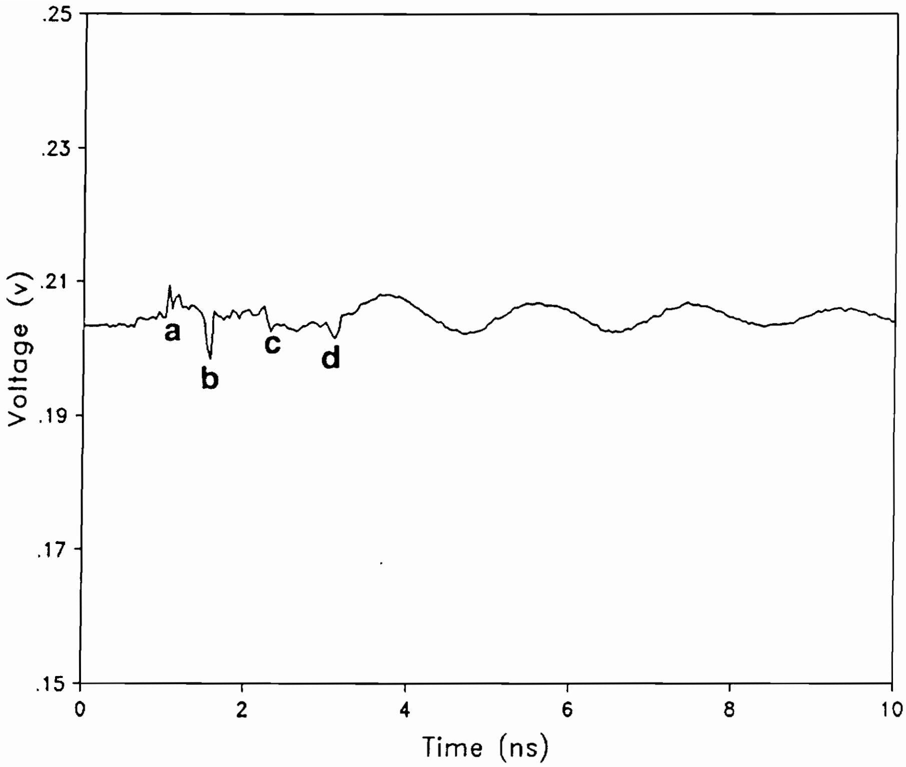

a __ Input connector
b __ Splitter
c __ Reversal junction
d __ Output connector

Figure 5.7 TDR Waveform of the Microstrip Balun When Two Output Grounds Are Not Connected to Each Other

The field propagated in this mode is often referred in the literature as that due to the ground currents initiated by the phase reversal.

Understanding the physical nature of the phase reversal junction leads to a physical explanation of the TDR responses. In case 1, the DC component is actually shorted through the connected grounds. The AC component needs certain time to travel through the shorting loop, exhibiting a decaying curve in the time domain. In this case, the slope of such a decay is a function of the length of the extended cables. The lower cutoff frequency in the frequency domain is related to the slope of the decay in the time domain. The slope is described by relation $\exp(-t/\tau)$, where τ is a decaying constant. Then, the lower cutoff frequency is determined by the relation $f = 1/(2\pi\tau)$. Therefore, the longer the extended cable, the slower the slope of the decay, and thus the lower the cutoff frequency. At the extreme of infinite length, the lower cutoff can be extended to DC. For a 3-foot long cable, the lower cutoff frequency is computed 2.46 MHz.

In case 2, although the cables are matched by 50 Ω terminations, the extra high impedance lines are in an open state. Under such a mismatch condition, the high impedance lines cause multi-reflections, seen as damped oscillations. The period of the oscillation is a function of the length of the high impedance lines. It is understandable that no decaying curve is observed because there no shorting loop.

The drop in the characteristic impedance occurs immediately after the phase reversal junction. This can be explained by the loading of the leakage fields into the high impedance "common mode" lines. The parallel combination of the high impedance lines and the negative phase line produce the lower impedance level observed in the TDR waveform.

Based on the analysis above, one can deduce that the phase reversal junction is where the negative polarity line couples with the two high impedance "common mode" lines. The geometrical discontinuities at the junction can be modeled as additional L and C components.

5.5. Modeling Results and Discussions

Combining the physical analysis of the discontinuities encountered through the transmission paths, an initial model for the microstrip line balun can be proposed. Such model is illustrated in Figure 5.8. This network model is converted into a computer file (see Appendix A), where MTCAP is used to simulate the model. As described in Section 5.2., the simulation process is an iterative one, involving tremendous work to adjust components values of the model, in order to match the simulated waveform to the measured waveform. The final match of the simulated waveform and the measured waveform is shown in Figure 5.9. The best component values in the model are obtained and listed in Table 5.1. Observing Figure 5.9, one can notice that the match of the two waveforms is not perfect. The extent to which the two waveforms are matched determines the accuracy of the obtained model.

The characteristic impedances of the extra coupling transmission lines can be determined using a computer software package called ANSOFT[23]. The basic idea to compute the impedances using ANSOFT is to compute the static capacitance among the associated conductors. The impedance can be then calculated using the relation,

$$Z0 = \eta_0 \frac{\sqrt{\epsilon\ \ \epsilon_0}}{C} \tag{24}$$

where $\eta_0 = 377\ \Omega$ is the intrinsic impedance of free space. C is the static capacitance. ϵ_r is the effective dielectric constant. ϵ_0 is the dielectric constant in free space. The cross section for the simulation to obtain the capacitance is shown Figure 5.10. The potential distribution is also seen from the Figure. The capacitance between conductor 1 and conductor 4 is 12.3 pf, giving rise to 318 Ω characteristic impedance.

It is interesting to verify the model obtained by the time domain technique in the frequency domain. Ideally, the results from the two domains should be in good agreement. The S-parameters measurements are achieved by conducting measurements on the balun using the HP-8510 Vector Network Analyzer as described earlier. The frequency domain simulation of the network model is conducted using PSpice[24] computer package (PSpice file is listed in Appendix B). The simulated result and the measured result are shown in Figure 5.11 for comparison purpose. It is seen that the matching is not as good as that in time domain. There exist some extensive dips and spikes. These dips and spikes may

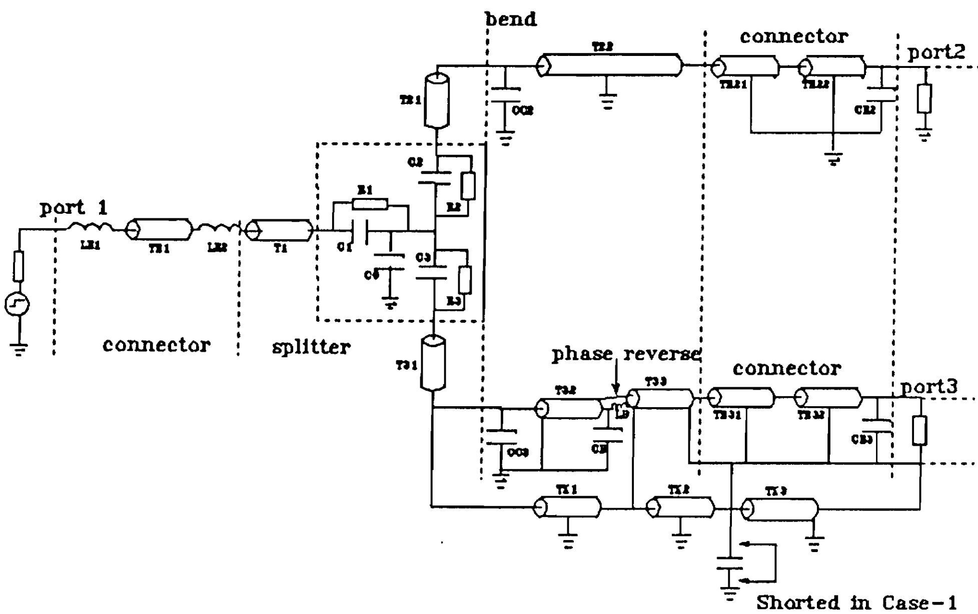

Figure 5.8 Microstrip Balun Network Model

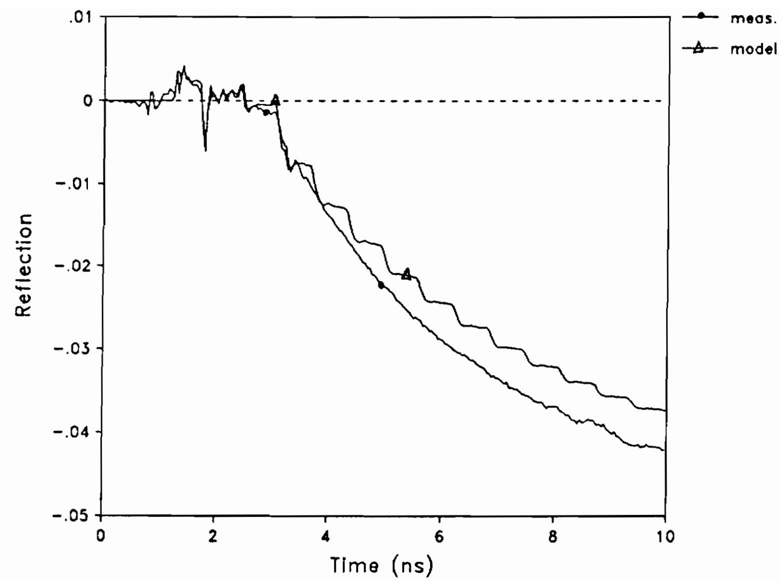

a) When two output grounds are connected

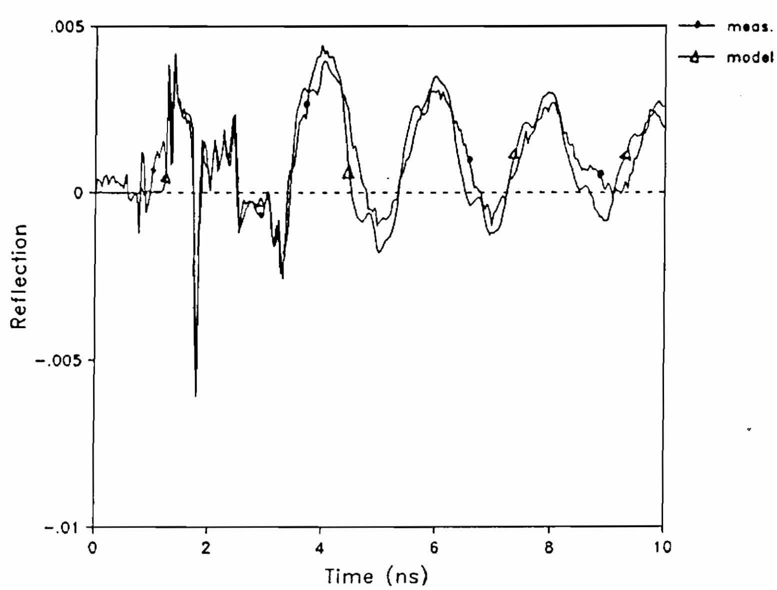

b) When two output grounds are not connected

Figure 5.9 Comparison of the MTCAP and the Experiment Waveforms

Table 5.1 Network Model Components for Microstrip Balun

	initial value	final value
LE1	0.355	0.255
TE1	46.6, 0.0585	48.6,0.0585
LE2	0.135	0.105
T1	50.0, 0.150	51.27,0.150
R1	16.67	17.37
C1	0.012	0.012
C0	0.36	0.33
R2	16.67	16.67
C2	0.012	0.012
T21	50.0,0.132	51.27,0.132
CC2	0.065	0.075
T22	50.0,0.528	51.27,0.528
TE21	46.5,0.048	46.5,0.048
TE22	51.5,0.040	51.5,0.040
CE2	0.105	0.105
R3	16.67	16.87
C3	0.012	0.012
T31	50.0,0.132	50.27,0.132
CC3	0.065	0.075
T32	50.0,0.223	51.27,0.223
LB	0.001	0.071
CB	0.200	0.250
T33	50.0,0.300	51.27,0.300
TE31	49.5,0.048	49.5,0.048
TE32	54.0,0.040	54.0,0.040
CE3	0.105	0.105
TX1	735,0.355	1000,0.355
TX2	318,0.300	350,0.300
TX3	318,0.145	380,0.145

Note: capacitor —— pf
resistor —— Ω
inductor —— nH
transmission line: impedance — Ω, delay — ns

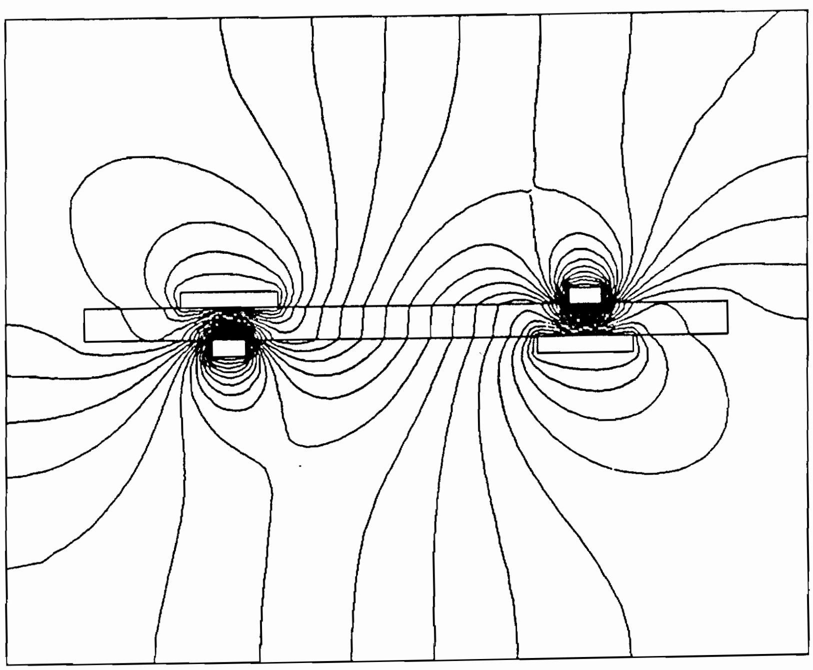

Figure 5.10 Potential Distribution of the Microstrip Balun Cross Section

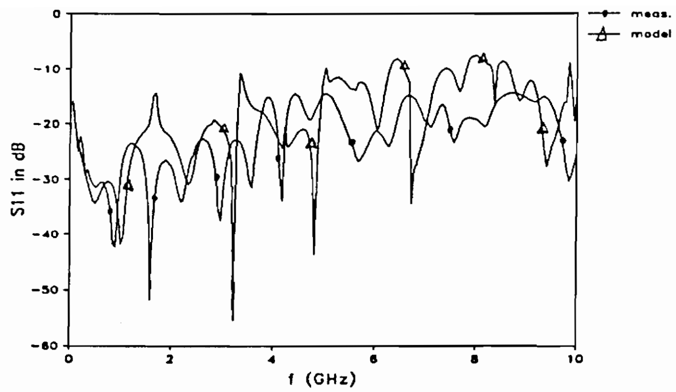

a) S11 versus frequency

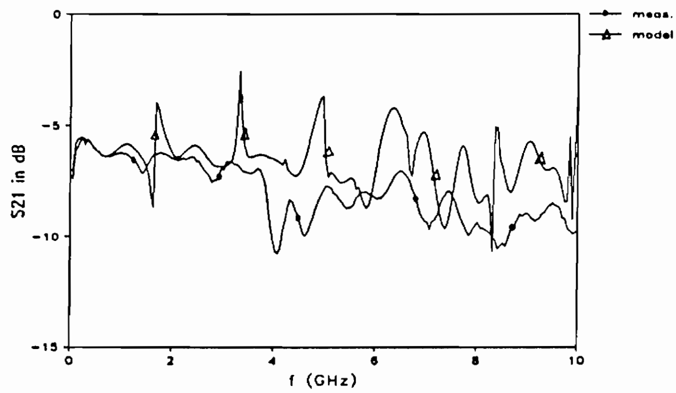

b) S21 versus frequency

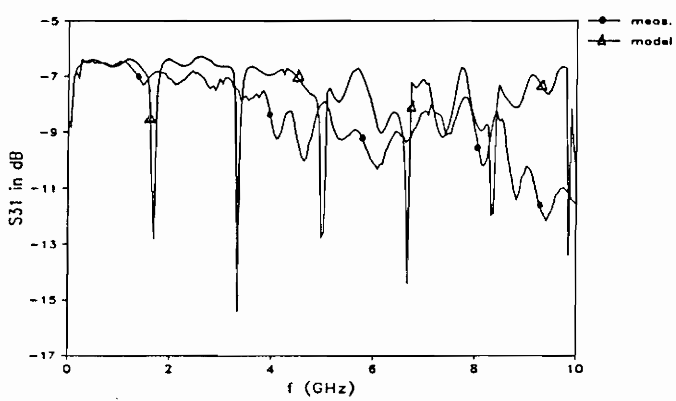

c) S31 versus frequency

Figure 5.11 Comparison of the PSPICE and the Experiment Waveforms When Two Output Grounds Are Connected to Each Other

be due to discrepancy in the model causing singularity in PSpice simulation.

It should be pointed out that the network model obtained is not unique. As an example, another network model can be proposed, as shown in Figure 5.12. This model is much simpler than the previous one. The model is based on the observation of the TDR waveforms with different lengths of extended cables beyond the output ports. If the shorting loop is considered as part of the balun's model, it can be modeled as inductors which are connected between the signal conductor and the ground. The values of the inductors are determined by the lengths of the extended cable. There are three inductors in shunt with the ground. Accounting for the effect of the high impedance lines, the value of the characteristic impedance after the reversal junction results from the parallel combination of 50 Ω with the characteristic impedance of the high impedance lines. The simulated waveforms in the time domain and in the frequency domain shown in Figures 5.13 and 5.14, respectively. However, there is one major disagreement between the simulated waveform and the experimental result in this model. Since the longer the extended cable, the larger the inductance value and the slower the curve decaying, at the extreme of infinite length extended cable, the inductors act like open circuits. The simulation of the model without the inductors shows a flat curve with no decay beyond the output ports. However, the experimental curve shows a damped oscillation. The comparison of the two waveforms are shown in Figure 5.15. Practically, the case of the infinite length extension does not exist because the balun is absolutely used with other devices or systems, which provide a finite extension. Therefore, the proposed model is acceptable for practical applications.

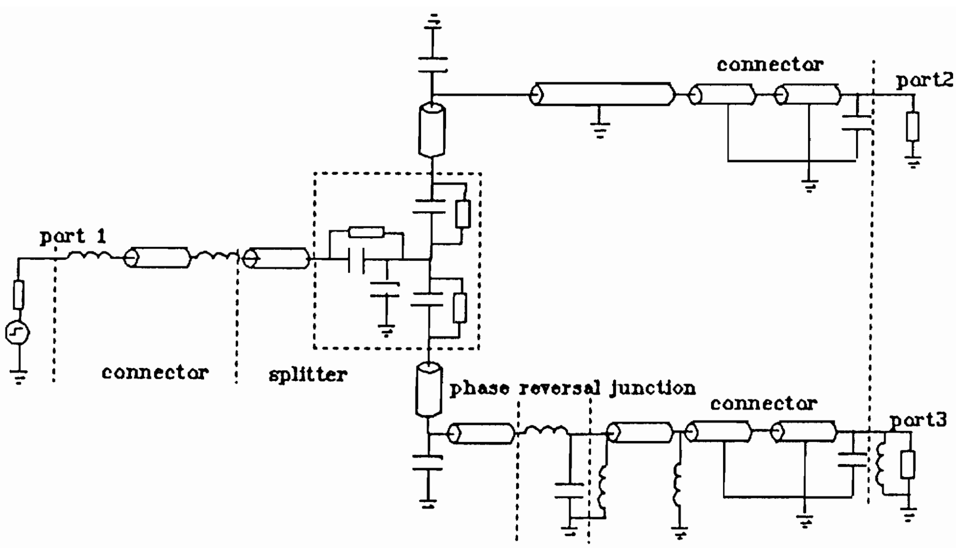

Figure 5.12 Alternative Network Model for the Microstrip Balun

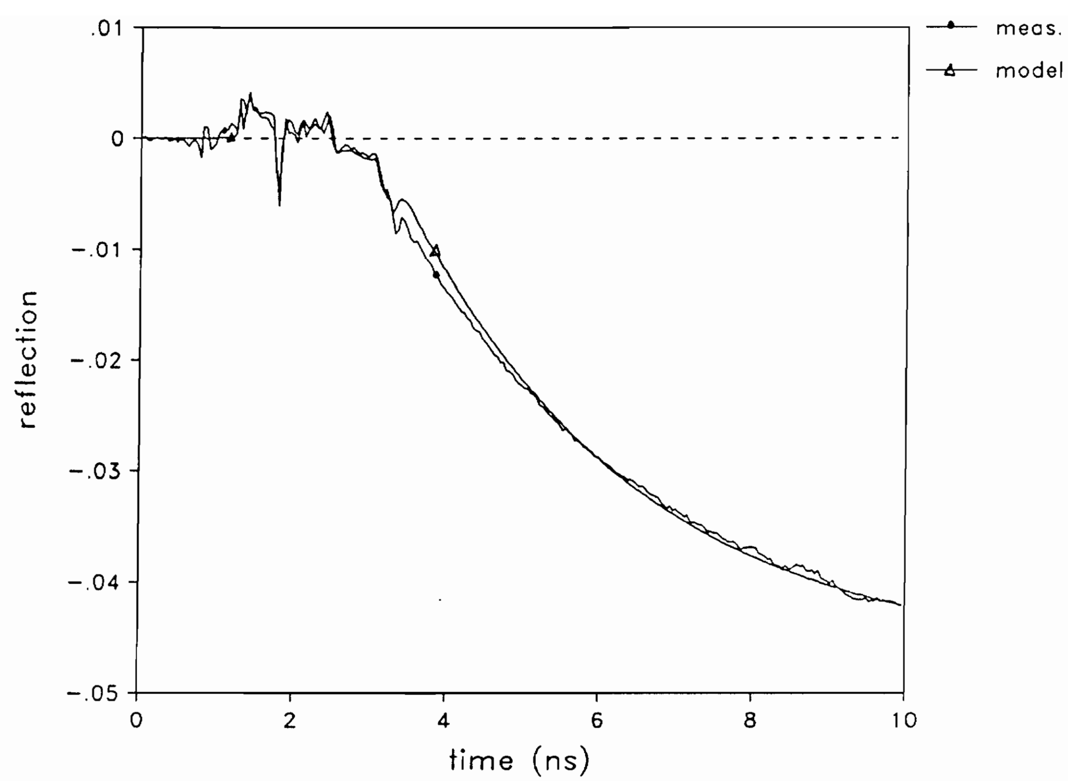

Figure 5.13 Comparison of the MTCAP and the experiment waveforms When Two Output Grounds Are Connected to Each Others

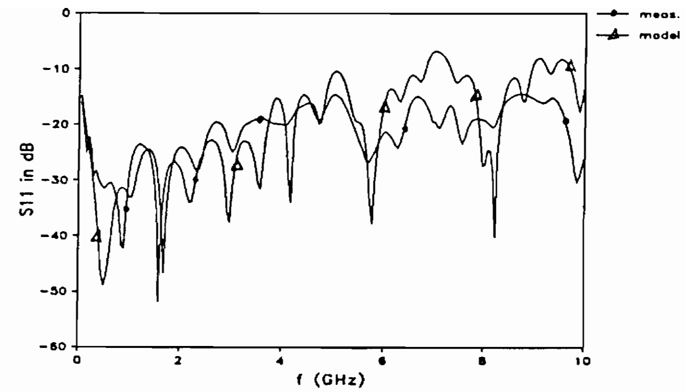

a) S11 versus frequency

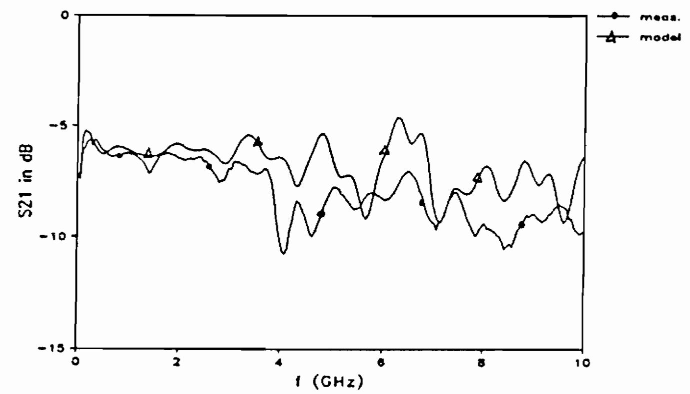

b) S21 versus frequency

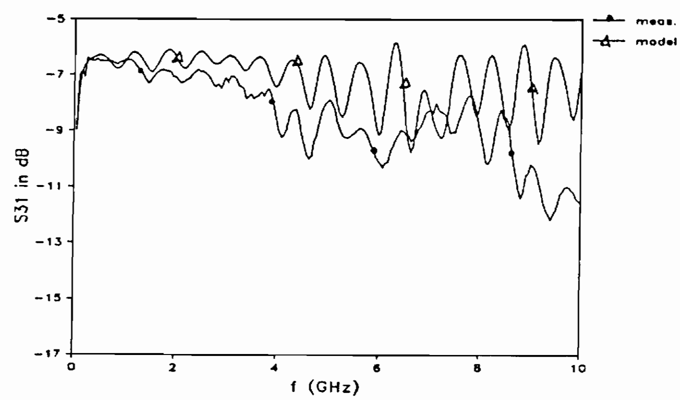

c) S31 versus frequency

Figure 5.14 Comparison of the PSPICE and the Experiment Waveforms When Two Output Grounds Are Connected to Each Others

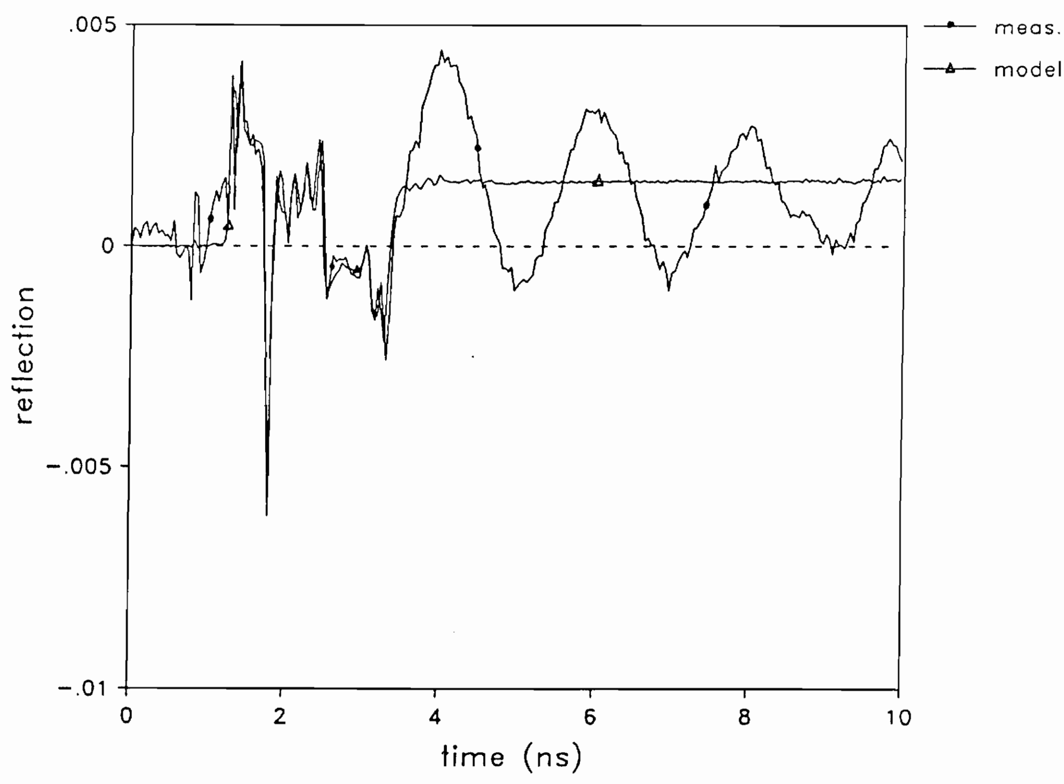

Figure 5.15 Comparison of the MTCAP and the Experiment Waveforms When Two Output Grounds Are Not Connected to Each Other

5.6. Conclusion

Time domain modeling technique is introduced in this chapter. The technique is based on analysis of the physical nature of the device to be modeled, leading to an initial model. Discontinuities through the transmission path are modeled as lumped and/or distributed R, L, C, and transmission lines as well as their combination of a series or shunt connections. Simulation of the initial model is conducted by using MTCAP to result in a waveform in time domain. The waveform is then compared with the measured TDR match is obtained.

This technique is applied to modeling of the microstrip line balun. Four significant discontinuities existing in the transmission path need to be modeled. The SMA connectors are modeled as an L, C, and a transmission line network, which may vary from time to time, depending on a specific case. The chip resistors in the power splitter are modeled as resistance with a capacitor in parallel and two capacitors in shunt, neglecting the effect of inductance. The 90-degree bend is modeled as a capacitor in shunt with the transmission line. Since the leakage fields, excited by the phase reversal junction, are propagated via two high impedance transmission lines, the junction is modeled as a transmission line network with additional R, L, and C. The simulation of the assumed model gives rise to good matching to the TDR waveform obtained by the time domain measurement of the balun, being proved to be adequate and acceptable. The resulting model is also verified in the frequency domain. Although the matching in frequency domain is not as good as that in the time domain, one can reasonably accept such treatment when ignoring the singularity in the simulation process.

CHAPTER VI

CONCLUSION

Design, fabrication using the hybrid technology, characterization and modeling using time domain and frequency domain techniques constitute the research work in this thesis. The motivation to conduct the research is to fulfill the practical requirements of a wideband and small size balun used for a microwave probe of a TDR measurement instrument. A review covering the various existing baluns indicates a vital necessity to conduct the research work involved in this thesis in order to meet specific applications.

Although an RF transformer balun possesses an advantage of small size, its bandwidth is limited due to the poor frequency characteristics of the materials in both low and high frequency ranges. The wideband balun with a bandwidth from 5 kHz to X band exhibits an excellent performance. However, it has relatively large size, which prohibits its application in an environment of a compact instrument. It is known that planar transmission lines provide advantages of wideband frequency performance, ease of realization, small size, and low cost. Therefore, a wideband microwave balun can be realized using planar transmission line approach.

Commonly used planar transmission lines include microstrip line and coplanar line. A microstrip line balun is proved to possess better performance than a coplanar line balun due to the difference in their field configurations. When geometrical discontinuities occur, the microstrip line introduces less field disturbance because of the fact that the field propagation is confined between two conductors. The design considerations of a microstrip line balun involve designs of a 50 Ω microstrip transmission line, a 6-dB power splitter, and a phase reversal junction. The 6-dB power splitter consists of three 16.67 Ω chip commercial resistors. The phase reversal junction is realized by manipulating geometry of a smooth tapered transition.

The microstrip line balun is fabricated on a 3" x 4" double-sided copper-cladded Teflon-Ceramic composite board using chemical etching method. This method is simple in processing and suitable for experimentation. The balun is measured using time domain techniques including TDR and TDT measurements and frequency domain techniques including S_{11} and S_{21} (S_{31}) measurements. The measurement results indicate that the 3 dB bandwidth of the balun is of the order of 5 GHz. Since the lowest frequency possible with the measuring instrument is 45 MHz, the lower cutoff frequency of the balun is calculated from the decaying constant of the TDT curves in time domain measurements. The value of the low cutoff frequency is equal to 2.46 MHz assuming that a 3-foot long testing cable is attached. Within the frequency range from 2.46 MHz to 5 GHz, S_{11} is below -20 dB. High frequency performance of the balun is determined by the bandwidth of the microstrip transmission line, the bandwidth of the splitter, and the bandwidth of the phase reversal junction.

The higher the upper cutoff frequencies of these three elements, the higher the upper cutoff frequency of the balun. The low frequency performance is determined by the standing waves produced by the propagation of the ground currents as a result of the phase reversal junction. These ground currents can be impeded, weakened or absorbed by allowing a long length of uniform cable on either side of the junction to eliminate possible standing waves.

The modeling and characterization, work of the microstrip line balun involves modeling of the discontinuities through the whole transmission paths. The modeling techniques used for modeling are based on time domain techniques. The techniques consist of three steps, which are: a) acquiring a TDR reflected waveform from the device and a reflected waveform from the reference plane, b) devising an initial network model represented by lumped circuit elements and distributed elements, and c) simulating the initial model using MTCAP and comparing the simulated waveform with the measured TDR waveform in an iterative manner until a good match is reached.

The initial network model is based on knowledge of the physical nature of the elements and structure details of the device as well as knowledge of time domain behaviors of various circuit elements. There are four significant discontinuities through the transmission path. The discontinuities include MELJ connectors for transition from coaxial to planar transmission lines, 6-dB power splitter, 90° bends, and phase reversal junction. The MELJ connectors with transition is modeled as a combination of a delay transmission line, an inductor and a capacitor. The model of the splitter contains resistances, and capacitances. The 90-degree bend is modeled as a capacitor in shunt with the ground conductor, omitting the effect of inductance.

Modeling of the phase reversal junction constitutes most of the work involved. The phase reversal junction excites leakage fields. The leakage fields are propagated via two high impedance transmission lines, which are formed through the two arms of the balun. The modeling of the phase reversal junction is considered as two different cases in terms of terminating situations. Case 1 is referred to the situation where two grounds of the output ports are connected to each other through the testing cable and then the measuring system. In this case, the TDR response starts to decay at a certain point of time until a saturated value is reached. Case 2 is the situation in which two grounds of the output ports are not connected, but the output ports are 50 Ω terminated. The TDR response exhibits a damped oscillation in case 2. The phase reversal junction is then modeled in a network containing inductors, capacitors, and lossless transmission lines. The difference between case 1 and case 2 in the model is represented by a small capacitor, which is shorted in case 1, while it is connected to ground in case 2.

Based on the analysis of the physical natures of the balun, a network model represented by R's, L's, C's, and transmission lines is proposed for simulation by MTCAP. Comparison of the simulation with experimental results and iterative process to modify the element values result in the final model of the balun, which represents the balun's operation performances.

References

[1] W. L. Stutzman, G. A. Thiele, « Antenna Theory and Design », John Wiley & Sons, Inc., pp.219, 1981.

[2] N. Nishizuka, et al, « Design of a Very-Wide-Band Transformer », IEEE Trans. on Components, Hybrids, and Manufacturing Technology, Vol. 11, No. 2, pp.191-194, June 1988.

[3] N. E. Lindenblad, « Television Transmitting Antenna for Empire State Building », RCA Rev., Vol. 3, pp.387-408, April 1939.

[4] N. Marchand, « Transmission Line Conversion Transformers », Electronics, Vol. 17, PP.142-145, December 1944.

[5] W. K. Roberts, « A New Wide-Band Balun », Proc. IRE, Vol. 45, pp.1628-1631, December 1957.

[6] H. G. Oltman, Jr., « Analysis of the Compensated Balun », Rantec Corp., Calif., Tech. Rept., May 1961.

[7] J. W. McLaughlin, et al, « A Wide-Band Balun », IRE Trans. on Microwave Theory and Techniques, Vol. MTT-6, pp.314-316, July 1958.

[8] G. Oltman, « The Compensated Balun », IEEE Trans. on Microwave Theory and Techniques, Vol. MTT-14, No. 3, pp.112-119, March 1966.

[9] R. Bawer, et. al, « A Printed Circuit Balun for Use with Spiral Antennas », IRE Trans. on Microwave Theory and Techniques, Vol. MTT-8, pp.319-325, May 1960.

[10] G. J. Laughlin, « A New Impedance-Matched Wide-Band Balun and Magic Tee », IEEE Trans. on Microwave Theory and Techniques, Vol. MTT-24, No. 3, pp.135-141, March 1976.

[11] B. Edward, et al, « A Broadband Printed Dipole with Integrated Balun », Microwave Journal, pp.339-344, May 1987.

[12] S. S. Bharj, et al, « Integrated Circuit 2-18 GHz Balun », Applied Microwave, pp. 110-119, November/December, 1989.

[13] Picosecond Pulse Labs Application Note, « Picosecond Pulse Labs », P.O.Box 44, BOULDER, COLORADO, 80306, USA, (303)443-1249, February, 1987.

[14] ANZAC, « RF and Microwave Components », 80 Cambridge Street, Burlington, Mass. 01803, (617)273-3333, pp.230

[15] A. A. Riad, et al, « Thick Film Coplanar Strip and Slot Transmission Lines For Microwave and Wideband

Integrated Circuits », <u>International Journal For Hybrid Microelectronics</u>, Vol. 5, No. 2, pp. 18-21, 1982.

[16] I. J. Bahl, et al, « A Designer's Guide to Microstrip Line » <u>Microwaves</u>, Vol. 16, No. 5, pp.174-182, May, 1977.

[17] K. C. Gupta, Ramesh Garg, I. J. Bahl, <u>« Microstrip Lines and Slotlines »</u> ARTECH HOUSE, INC., PP.275, 1979.

[18] EEsof, « LineCalc », EEsof, Inc., 31194 La Baya Drive, Westlake Village, CA 91362, May 1986.

[19] S. M. Riad, « Instructional Opportunities Offered by the Time-Domain Measurement Technology », Chapter 3, E. K. Miller, <u>« Time-Domain Measurements in Electromagnetics »</u>, VAN NOSTRAND ERINHOLD COMPANY, New York, 1986.

[20] Hewlett-Packard Application Note, « Vector Measurements of High Frequency Networks », pp.A-4, August 1, 1987.

[21] S. M. Riad, et al, « The Modified Transient Circuit Analysis Package (MTCAP) », Department of Electrical Engineering, Virginia Polytechnic Institute and State University, April 1988.

[22] K. M. Fidanboylu, et al, « A New Approach to Planar Structure Characterization Using Time Domain

Techniques », 31st ARFTG Conf. Digest, New York, New York, USA, pp.19-28, May 1988.

[23] Ansoft Corporation, « ANSOFT », University Technology Development Center, 4516 Henry Street, Pittsburgh, PA 15213, (412)683-4846, January, 1989.

[24] MicroSim Corporation, « PSpice », 23175 La Cadena Drive, Laguna Hills, CA 92653, July, 1987.

Appendix A

Circuit file for microstrip balun:

```
  B1, N(1,0), VXTS1 = 1, NINPTS = 256, NAME = OPENS.DAT
  B2, N(1,2), RRS = 50.0
C*************************
  B3, N(2,3), LL10 = 0.2550E-09, L0 = 0.0
  B4, N(3,0), TLINDEL10 = 0.0285E-09, R0 = 48.6, N < 4,0 >
  B5, N(4,5), LL10 = 0.105E-09, L0 = 0.0
  B6, N(5,0), TLINDEL11 = 0.1800E-09, R0 = 51.27, N < 6,0 >
  B7, N(6,7), RR11 = 17.37
  B8, N(6,7), CC11 = 0.012E-12, C0 = 0.0
  B9, N(7,0), CC01 = 0.330E-12, C0 = 0.0
  B10, N(7,8), RR12 = 16.67
  B11, N(7,8), CC12 = 0.0120E-12, C0 = 0.0
  B12, N(8,0), TLINDEL21 = 0.132E-09, R0 = 51.27, N < 9,0 >
  B13, N(9,0), CCC2 = 0.075E-12, C0 = 0.0
  B14, N(9,0), TLINDEL22 = 0.528E-09, R0 = 51.27, N < 10,0 >
  B15, N(10,0), TLINDELE21 = 0.048E-09, R0 = 46.5, N < 23,0 >
  B16, N(23,0), TLINDELE22 = 0.040E-09, R0 = 51.5, N < 24,0 >
  B17, N(24,0), CCE2 = 0.105E-12, C0 = 0.0
  B18, N(24,0), RRO2 = 50.0
  B19, N(7,11), RR13 = 16.87
  B20, N(7,11), CC13 = 0.0120E-12, C0 = 0.0
  B21, N(11,0), TLINDEL31 = 0.1320E-09, R0 = 50.27, N < 12,0 >
  B22, N(12,0), CCC3 = 0.075E-12, C0 = 0.0
  B23, N(12,0), TLINDEL32 = 0.070E-09, R0 = 51.27, N < 13,0 >
  B24, N(13,0), CCB1 = 0.105E-12, C0 = 0.0
  B25, N(13,0), TLINDEL33 = 0.075E-09, R0 = 51.27, N < 14,0 >
  B26, N(14,0), CCB2 = 0.175E-12, C0 = 0.0
  B27, N(14,0), TLINDEL34 = 0.078E-09, R0 = 54.2, N < 15,0 >
  B28, N(15,0), CCB3 = 0.250E-12, C0 = 0.0
  B29, N(15,16), LLB3 = 0.071E-09, L0 = 0.0
  B30, N(16,0), TLINDEL35 = 0.265E-09, R0 = 51.27, N < 17,18 >
  B31, N(18,17), TLINDEL36 = 0.035E-09, R0 = 54.9, N < 19,20 >
  B32, N(19,20), TLINDELE31 = 0.048E-09, R0 = 49.5, N < 21,20 >
  B33, N(21,20), TLINDELE32 = 0.040E-09, R0 = 54.0, N < 22,20 >
  B34, N(22,20), CCE3 = 0.105E-12, C0 = 0.0
  B35, N(15,0), TLINDELX1 = 0.355E-09, R0 = 1000, N < 11,0 >
  B36, N(16,0), TLINDELX2 = 0.300E-09, R0 = 350, N < 17,0 >
  B37, N(17,0), TLINDELX3 = 0.140E-09, R0 = 380, N < 20,0 >
C  B38, N(17,0), CCX1 = 0.0100E-12, C0 = 0.0
  B38, N(17,0), RRX1 = 0.0
  B39, N(22,20), RRO3 = 50.0
CCCCCCCCCCCCCCCCCCCCCCCCCCCCCCCCCCCCCCCCCCCCCCCC
```

```
    TMAX = 10.0000000E-09
    TMIN = 0.00000000E-09
    NUMPTS = 256
    PRINT NODE VOLTAGES = 3:2,24,22
    WAVEFORM COMP = 2, WINDOW = 0,2,1,256, WAVEFORM NAME = S11SHORT.DAT
END
```

Appendix B

```
*SIMULATED MODEL FOR MICROSTRIP BALUN CIRCUIT MODEL
*PSPICE SIMULATION DATA FOR CALCULATING S11 AND S21
.AC LIN 201  45.0E+6  10.00E+9
RS   1 0 50
I1   1 0 AC   -20.0E-3
E11  10 0 1 0 2
V11  10 11 AC 1
R11 11 0 1
XBALUN 1 2 3 4 BALUN
RL1 2 0 50
E21 21 0 2 0 2
R21 21 0 1
RL2 3 4 50
E31 31 0 3 4 2
R31 31 0 1
**************************
.SUBCKT  BALUN        2 24 22 20
L10 2 3 0.2550E-09
T10 3 0 4 0 Z0=48.6 TD=0.0585E-09
L11 4 5 0.1050E-09
T11 5 0 6 0 Z0=51.27 TD=0.150E-09
R11 6 7 17.37
C11 6 7 0.012E-12
C10 7 0 0.330E-12
R12 7 8 16.67
C12 7 8 0.012E-12
T21 8 0 9 0 Z0=51.27 TD=0.132E-09
CC2 9 0 0.075E-12
T22 9 0 10 0 Z0=51.27 TD=0.528E-09
TE21 10 0 23 0 Z0=46.5 TD=0.048E-09
TE22 23 0 24 0 Z0=51.5 TD=0.040E-09
CE2 24 0 0.105E-12
*RO2 24 0 50.0
R13 7 11 16.87
C13 7 11 0.012E-12
T31 11 0 12 0 Z0=50.27 TD=0.1320E-09
CC3 12 0 0.075E-12
T32 12 0 13 0 Z0=51.27 TD=0.070E-09
CB1 13 0 0.105E-12
T33 13 0 14 0 Z0=51.27 TD=0.075E-09
CB2 14 0 0.175E-12
T34 14 0 15 0 Z0=54.2 TD=0.078E-09
CB3 15 0 0.250E-12
LB3 15 16 0.071E-09
```

```
T35 16 0 17 18 Z0 = 51.27 TD = 0.265E-09
TE31 18 17 19 20 Z0 = 54.9 TD = 0.035E-09
TE32 19 20 21 20 Z0 = 49.5 TD = 0.048E-09
TE33 21 20 22 20 Z0 = 54.0 TD = 0.040E-09
CE3 22 20 0.105E-12
TX1 16 0 11 0 Z0 = 1000 TD = 0.355E-09
TX2 16 0 17 0 Z0 = 350 TD = 0.300E-09
TX3 17 0 20 0 Z0 = 380 TD = 0.145E-09
RX1 17 0 0.0001
*RO3 22 20 50.0
.ENDS BALUN
*****************************
.OPTIONS RELTOL = 0.0001 LIMPTS = 201
.PRINT AC VM(11) VP(11) VM(21) VP(21) VM(31) VP(31)
.PROBE
.END
```

VITA

Shu Lu was born in Guangzhou(Canton), People's Republic of China on December 19, 1962. In September 1980, she attended South China Institute of Technology, where she majored in semiconductor physics and devices. She earned her B.S. degree in July 1984. After graduation, she was hired as an engineer and worked on device testing for computer hardware in South China Computer Corporation, where she also involved in several software design projects. From September 1988, She began her graduate study in the Department of Electrical Engineering, Virginia Polytechnic Institute and State University, guided by both Dr. A. Elshabini-Riad and Dr. S.M. Riad.

Shu Lu is a student member of IEEE and a member of International Society of Hybrid Microelectronics (ISHM). She has co-authored one journal paper, published on Hybrid Circuit Technology and five conference papers.